Biogeosciences Discuss., 7, 111–164, 2010
www.biogeosciences-discuss.net/7/111/2010/

Biogeosciences Discussions

This discussion paper is/has been under review for the journal Biogeosciences (BG).
Please refer to the corresponding final paper in BG if available.

Influence of consumer-driven nutrient recycling on primary production and the distribution of N and P in the ocean

A. Nugraha, P. Pondaven, and P. Tréguer

Institut Universitaire Européen de la Mer (IUEM), Laboratoire des Sciences de l'Environnement Marin (LEMAR), UMR CNRS/UBO/IRD 6539, Technopole Brest-Iroise, Place Copernic, 29280 Plouzané, France

Received: 16 November 2009 – Accepted: 30 November 2009 – Published: 12 January 2010

Correspondence to: A. Nugraha (nugraha@univ-brest.fr)

Published by Copernicus Publications on behalf of the European Geosciences Union.

Abstract

In this study we investigated the impact of consumer-driven nutrient recycling (CNR) on oceanic primary production and the distribution of nitrogen (N) and phosphorus (P) in the deep ocean. For this purpose, we used and extended two existing models: a 2-box model of N and P cycling in the global ocean (Tyrrell, 1999), and the model of Sterner (1990) which formalised the principles of CNR theory. The resulting model showed that marine herbivores may affect the supply and the stoichiometry of N and P in the ocean, thereby exerting a control on global primary production. The predicted global primary production was higher when herbivores were included in the model, particularly when these herbivores had higher N:P ratios than phytoplankton. This higher primary production was triggered by a low N:P resupply ratio, which, in turn, favoured the P-limited N_2-fixation and eventually the N-limited non-fixers. Conversely, phytoplankton with higher N:P ratios increased herbivore yield until phosphorus became the limiting nutrient, thereby favouring herbivores with a low P-requirement. Finally, producer-consumer interactions fed back on the N and P inventories in the deep ocean through differential nutrient recycling. In this model, N deficit or N excess in the deep ocean resulted not only from the balance between N_2-fixation and denitrification, but also from CNR, especially when the elemental composition of producers and consumers differed substantially. Although the model is fairly simply, these results emphasize our need for a better understanding of how consumers influence nutrient recycling in the ocean.

1 Introduction

Owing to their scarcity in the well-lit surface layers, nitrogen (N) and phosphorus (P) frequently limit primary production in the ocean (Ryther and Dunstan, 1971; Howarth, 1988; Vitousek and Howarth, 1991; Downing, 1997; Tyrrell, 1999; Wu et al., 2000). As such, the processes governing the biogeochemistry of these two elements have been of interest for a long time and are still actively investigated (e.g. Redfield et al., 1963;

BGD

7, 111–164, 2010

Dugdale and Goering, 1967; Tyrrell, 1999; Karl et al., 2001; Arrigo, 2005; Slomp and Van Cappellen, 2007; Hutchins and Fu, 2008).

These key processes include the delivery of N and P from the continents and atmosphere, their redistribution via ocean circulation, and their cycling within the ocean and sediments. Riverine inputs and atmospheric deposition contribute to 46–57% of the total N inputs to the ocean (Gruber and Galloway, 2008). N_2-fixation is an additional significant source of new N to the ocean, especially in oligotrophic gyres where this process contributes approximately 40–52% of new-N inputs to the well-lit surface layer (Codispoti et al., 2001; Gruber, 2004). Phosphorus is mainly delivered to the ocean through rivers (94% of the inputs) as a product of continental weathering, while the eolian flux contributes for the remaining 6% of the total phosphorus flux at present day (Compton et al., 2000).

Once in the ocean, it has long been recognised that biological processes exert a control on N and P cycles (Redfield et al., 1963). Dissolved inorganic N and P are taken up and converted into organic matter by photosynthetic autotrophs in the euphotic zone. Organic N and P are then transferred, either to higher trophic levels in the food web or into the deep ocean. Eventually N and P are remineralised or buried in sediments.

In their seminal work, Redfield et al. (1963) found that the stoichiometry of N and P in the bulk plankton biomass converges on a mean ratio of 16N:1P, the so-called Redfield ratio, which closely matches that of the dissolved inorganic pool in the ocean. Based on these observations, Redfield et al. (1963) suggested that marine organisms imprint the biogeochemistry and the distribution of these major elements in the ocean. This finding profoundly influenced the field of marine biogeochemistry over the decades that followed.

The Redfield ratio is still used as a scaling factor within models to derive biological-driven fluxes of elements in the ocean (e.g. Arrigo, 2005; Sarmiento and Gruber, 2006). However, debate remains about the mechanisms which drive the stoichiometry of these elements in the ocean, and its resulting influence on primary productivity (e.g. Tyrrell, 1999; Lenton and Klausmeier, 2007). Significant deviations from

Redfield stoichiometry have been reported at different scales, ranging from the organism (e.g. Geider and La Roche, 2002; Quigg et al., 2003; Klausmeier et al., 2004) to the ecosystem (e.g. Karl et al., 2001). Karl et al. (2001) found for example that, in the north Pacific gyre, the N:P ratio in the particulate and dissolved organic pools shows variations in the euphotic zone from $<5:1$ to $>50:1$, averaging 19.4:1 (POM) and 19.6:1 (DOM).

Despite these deviations, the stoichiometry of dissolved inorganic N and P in the ocean is nearly constant over large spatial scales (Redfield et al., 1963). This suggests that various processes operate in the surface or the deep ocean to both drive and buffer deviations from Redfield stoichiometry. Several mechanisms capable of this have been identified, for example, the balance between nitrogen fixation and denitrification (Redfield et al., 1963), the existence of a wide range of optimal N:P ratios in phytoplankton (Quigg et al., 2003; Klausmeier et al., 2004), and variations in marine redox conditions that affect the sedimentary sequestration of P (Van Cappellen and Ingall, 1996).

Here we investigate how the stoichiometry of consumer-driven nutrient recycling (Sterner, 1990) may influence primary production and the distribution of N and P in the ocean. We have done this because producer-consumer interactions have been shown to exert a control on nutrient cycling and other various ecosystem functions in numerous freshwater systems (Elser and Urabe, 1999; Sterner and Elser, 2002). The great extent of herbivory in marine systems (Calbet, 2001; Cebrián, 2004; Landry and Calbet, 2004) suggests that these interactions may also be important in the ocean, as has been previously suggested by Corner and Davies (1971). Additionally, the elemental composition of herbivores is not only different from that of their algal food (Sterner, 1990; Sterner et al., 1992; Elser and Urabe, 1999), but it is also often homeostatic, irrespective of the elemental composition of their prey (Sterner et al., 1992; Elser and Urabe, 1999). Homeostatic regulation of whole body elemental composition is maintained by releasing elements which are in excess to requirements, while more efficiently retaining limiting elements. These principles form the basis of the "Consumer-driven

nutrient recycling theory", hereafter called CNR (Elser and Urabe, 1999; Sterner and Elser, 2002; Pilati and Vanni, 2007).

Owing to the low gross growth efficiency (GGE) of aquatic herbivores (~20–40%), most of their ingested food is either egested as particulate organic matter (POM) or excreted as dissolved products (Miller and Landry, 1984; Straile, 1997; Besiktepe and Dam, 2002). The fate of the products released by herbivores, and their relative N:P ratio (known as "resupply ratio", Sterner, 1990), may significantly affect nutrient cycling in the ocean, which, in turn, may feed back on primary producers. To address the question of the possible contribution of CNR in driving the oceanic primary production and the distribution of N and P throughout the ocean, we extended and used two existing models, a 2-box model of N and P cycling in the global ocean (Tyrrell, 1999) and the model of Sterner (1990) that formalised the principles of CNR theory.

2 Model description

2.1 Model framework

The model described here combines and extends concepts from previous modelling studies (Sterner, 1990; Tyrrell, 1999). Tyrrell's model describes the cycling of reactive forms of N and P in a global ocean represented by two boxes, a surface box (0–500 m) and a deep box (500–3230 m) (Fig. 1). The vertical distributions of dissolved inorganic N and P are constrained by a constant amount of mixing (K), remineralisation of organic N and P in the surface and deep layers for phytoplankton (SR_0 and DR_0, respectively), denitrification (DN), and burial in sediments (SF). The constant amount of mixing parameterises ocean overturning, upwelling, and diffusion with a time scale of ~1000 yr (Broecker and Peng, 1982). The ecosystem focuses on autotrophic organisms with explicit competition between N_2-fixers (NF) and other algae (hereafter "non-fixers") (O) in the surface ocean. The former require only phosphate as they can convert N_2 gas into organic N. The latter require both nitrate and phosphate. A single

loss term represents all possible sources of natural mortality. This mortality term fuels an implicit detrital pool which is partly remineralised in the surface and deep boxes. The fraction which escapes remineralisation is lost from the system as burial in sediments. In the model presented here, the basic set-up of Tyrell's model is conserved.

In addition, we implemented an upper trophic level (herbivores) with homeostatic regulation of their N:P body content, following Sterner's (1990) approach (Fig. 1). Homeostatic regulation of N and P body content is taken into account by differentiating a GGE for N and P. GGE is classically defined as:

$$\mathrm{GGE}_i = \frac{I_i - (F_i + E_i)}{I_i}, \quad (1)$$

where I_i is the ingestion of the element i, and F_i and E_i are the release of this element as either faecal pellets or dissolved products. The release of dissolved N or P depends on the differences between the N:P stoichiometry of assimilated food and that of the organism. In other words, the element in excess to requirement will be released (excreted) in higher proportion than the other, while the accumulated fraction will be used for growth. This concept was formalised by Sterner (1990) by defining a different accumulation efficiency for N and P.

The model equations and parameterisations which combine these two model frameworks are detailed below.

2.2 Model formulation

There are seven state variables in the model. They correspond to N_2-fixers (NF), non-fixers (O), herbivores (H_1), surface phosphate (P_S), surface nitrate (N_S), deep phosphate (P_D), and deep nitrate (N_D) and are explained below. We will concentrate below on the main modifications made to Tyrrell's model.

BGD
7, 111–164, 2010

2.2.1 Phytoplankton (NF and O)

Phytoplankton are assumed to occur only in the surface ocean. As in Tyrell's model, the two phytoplankton competitors, NF and O, are included.

$$\frac{d\mathrm{NF}}{dt} = \mu'_{\mathrm{NF}} \frac{\mathrm{P_S}}{K_\mathrm{P} + \mathrm{P_S}} \mathrm{NF} - M_0 \mathrm{NF} \tag{2}$$

$$\frac{d\mathrm{O}}{dt} = \mu'_{\mathrm{O}} \min\left(\frac{\mathrm{P_S}}{K_\mathrm{P} + \mathrm{P_S}}, \frac{\mathrm{N_S}}{K_\mathrm{N} + \mathrm{N_S}}\right) \mathrm{O} - M_0 \mathrm{O} \tag{3}$$

Both phytoplankton equations are composed of two terms, a growth term and a loss term. The growth rates of NF and O are controlled using a Liebig's Law formulation consisting of a maximum growth rate (either μ'_{NF} or μ'_{O}) times a Michaelis-Menten term for nutrient uptake. The last term in the equations above is the loss term represented by a constant specific mortality rate (M_0) which covers all possible loss terms pathways from phytoplankton. Mortality for both types of phytoplankton is similar. This assumption implies that N_2-fixers are P-limited while non-fixers are N-limited (Tyrrell, 1999).

2.2.2 Herbivores

The herbivore mass balance is governed by three processes, the ingestion of food (phytoplankton), the release of products (faecal pellets and dissolved nutrients), and natural mortality (Fig. 2). Following an extended version of Sterner's (1990) approach, homeostatic regulation of the herbivore N and P body content is governed by three parameters, the assimilation efficiency β_1^{N} or β_1^{P}, the accumulation efficiency for nitrogen (a_N) or phosphorus (a_P), and the N:P ratio of either assimilated food (f) or herbivore (b). It should be noted that Sterner (1990) did not explicitly consider the assimilation efficiency and the production of faecal pellets or detritus due to sloppy feeding. In Sterner's model, f represents the N:P ratio of the resource itself, while f here is the N:P

ratio of the resource assimilated after ingestion and gut passage, the rest of the N and P being released as either detritus from sloppy feeding or as faecal pellets. This yields

$$b = f\frac{a_N}{a_P} \tag{4a}$$

with

$$f = R^i_{org}\frac{\beta^N_1}{\beta^P_1}. \tag{4b}$$

In Eq. (4b), R^i_{org} is the N:P ratio of phytoplankton, with i = NF or O. The value of a_N and a_P can be calculated according to two criteria (Fig. 3). The first case is when f<b. In this case, N is the limiting element for zooplankton growth and its accumulation efficiency is maximal, i.e. $a_N = L_m$. On the other hand, P is in excess compared to requirement, so that its accumulation efficiency is lower than that of N, i.e. $a_P = L_m f/b$. The second case is when f>b. In this case, nitrogen is in excess compared to requirement, and thus its accumulation efficiency is $a_N = L_m b/f$. Phosphorus is then the limiting element and its accumulation efficiency is maximal, i.e. $a_P = L_m$. The proportion of the element in excess to requirement, E_i, is release as dissolved material, i.e. $E_i = (1 - a_i)\beta_i I_i$.

By combining Eq. (1), the assimilation efficiency, β_i, and the accumulation efficiency, a_i, the GGE for each element is simply

$$GGE_i = a_i\beta_i. \tag{5}$$

Then the equation for zooplankton in terms of N units is,

$$\frac{dH_1}{dt} = \left\{\beta^N_1\varepsilon_0 M_0\left(a^{NF}_N NF + a^O_N O\right)\right\}\frac{SD}{SD + DD} - M_1 H_1, \tag{6}$$

where β^N_1 is the assimilation efficiency of N, ε_0 is the proportion of phytoplankton natural mortality (M_0) due to grazing, a^{NF}_N and a^O_N are the accumulation efficiencies of N

when herbivores feed on N_2-fixers (NF) or non-fixers (O), and M_1 is the natural mortality of herbivores. Because R^Z_{org} is constant, an explicit equation for zooplankton in term of P is not necessary. Finally, unlike phytoplankton, herbivores are assumed to vertically migrate, something that is parameterised here by assuming that their biomass is distributed between the surface (SD) and the deep layer (DD). This vertical distribution mainly affects the mass balance of dissolved nutrient through the proportions of detritus or dissolved products which are released by zooplankton in either the surface or the deep layer (see below).

2.2.3 Dissolved inorganic nitrogen and phosphorous

The rates of change of total dissolved N and P in the surface (N_S, P_S) are described by the equations below:

$$\begin{aligned}
\frac{dP_S}{dt} &= -\mu'_{NF}\frac{P_S}{K_P+P_S}\frac{NF}{R^{NF}_{org}} - \mu'_O \min\left(\frac{P_S}{K_P+P_S}, \frac{N_S}{K_N+N_S}\right)\frac{O}{R^O_{org}} \\
&+(1-\varepsilon_0)M_0 SR_0\left(\frac{NF}{R^{NF}_{org}}+\frac{O}{R^O_{org}}\right)+(1-\beta^P_1)\varepsilon_0 M_0\left(\frac{NF}{R^{NF}_{org}}+\frac{O}{R^O_{org}}\right)SR_1 \\
&+\left\{\beta^P_1\varepsilon_0 M_0\left(\left(1-a^{NF}_P\right)\frac{NF}{R^{NF}_{org}}+\left(1-a^O_P\right)\frac{O}{R^O_{org}}\right)\right\}SE_1 \\
&+\left\{M_1\frac{H_1}{R^Z_{org}}SR_1\right\}\frac{SD+DD}{SD}+K\frac{(P_D-P_S)}{SD}+\frac{RP}{SD}
\end{aligned} \tag{7}$$

$$\begin{aligned}
\frac{dN_S}{dt} &= -\mu'_O \min\left(\frac{P_S}{K_P+P_S}, \frac{N_S}{K_N+N_S}\right)O \\
&+(1-\varepsilon_0)M_0(NF+O)(SR_0-0.75DN) \\
&+(1-\beta^N_1)\varepsilon_0 M_0(NF+O)(SR_1-0.75DN) \\
&+\left\{\beta^N_1\varepsilon_0 M_0\left(\left(1-a^{NF}_N\right)NF+\left(1-a^O_N\right)O\right)\right\}(SE_1-0.75DN) \\
&+\{M_1 H_1(SR_1-0.75DN)\}\frac{SD+DD}{SD}+K\frac{(N_D-N_S)}{SD}+\frac{(AN+RN)}{SD}
\end{aligned} \tag{8}$$

The negative terms describe nutrient uptake by phytoplankton. The addition of nutrient to the surface layer is fuelled by the fraction of phytoplankton mortality which is not related to herbivore grazing (term 2 which includes cell lysis, sinking etc), the release of faecal pellets by herbivores (term 3), herbivore excretion (term 4), herbivore natural mortality (term 5), mixing (term 6), and external nutrient inputs (term 7). For both nutrients, a fraction of primary and of secondary production is remineralised in the surface layer (SR_0 and SR_1, respectively). Remineralisation is also accounted for by herbivores' excretion of dissolved products (SE_1). In addition, N is removed from the system by denitrification (DN). Finally, N_2-fixers and non-fixers have distinct N:P stoichiometry (R^{NF}_{org} and R^{O}_{org}, respectively).

The rates of change of total dissolved N and P in the deep ocean (N_D, P_D) are given by:

$$\begin{aligned}\frac{dP_D}{dt} &= (1-\varepsilon_0)M_0\left(\frac{NF}{R^{NF}_{org}}+\frac{O}{R^{O}_{org}}\right)\frac{SD}{DD}DR_0+(1-\beta^P_1)\varepsilon_0 M_0\left(\frac{NF}{R^{NF}_{org}}+\frac{O}{R^{O}_{org}}\right)\frac{SD}{DD}DR_1\\ &+\left\{\beta^P_1\varepsilon_0 M_0\left(\left(1-a^{NF}_P\right)\frac{NF}{R^{NF}_{org}}+\left(1-a^{O}_P\right)\frac{O}{R^{O}_{org}}\right)\right\}\frac{SD}{DD}DE_1\\ &+\left\{M_1\frac{H_1}{R^{Z}_{org}}DR_1\right\}\frac{SD+DD}{DD}-K\frac{(P_D-P_S)}{DD}\end{aligned} \quad (9)$$

$$\begin{aligned}\frac{dN_D}{dt} &= (1-\varepsilon_0)M_0(NF+O)\frac{SD}{DD}(DR_0-0.25DN)\\ &+(1-\beta^N_1)\varepsilon_0 M_0(NF+O)\frac{SD}{DD}(DR_1-0.25DN)\\ &+\left\{\beta^N_1\varepsilon_0 M_0\left(\left(1-a^{NF}_N\right)NF+\left(1-a^{O}_N\right)O\right)\right\}\frac{SD}{DD}(DE_1-0.25DN)\\ &+\{M_1H_1(DR_1-0.25DN)\}\frac{SD+DD}{DD}-K\frac{(N_D-N_S)}{DD}\end{aligned} \quad (10)$$

Nutrients enter into the deep ocean via the fraction of particulate organic matter (POM) remineralised is the deep layer (DR_0 and DR_1) and the excretion of nutrients that are in excess to requirement (DE_0 and DE_1). Denitrification (DN) removes dissolved organic N from this reservoir. Mixing processes (K) are also responsible for the transfer of both

nutrients from the deep box into the surface box. The fraction of organic material which escapes remineralisation, SF, leaves the system and is buried in the sediments.

2.3 Parameterization

Lists of parameters with their descriptions, units, and values are given in Table 1. We have split the model parameters into two groups, extended Tyrrell's model's and extended Sterner's model's parameters. All material units are expressed in moles, spatial dimensions are in meters, and time is in years. All fraction and efficiency terms are given as percentages and N:P ratios are dimensionless.

The physical characteristics of Tyrrell's model were conserved. These include the depth of surface and deep layers (SD and DD), total volume and surface area of the ocean (T_{vol} and T_{area}), the ocean mixing coefficient (K), riverine input of P (RP) and N (RN) and atmospheric inputs of N (AN).

The biological parameters of primary producers in our model were mostly derived from Tyrell's model. For example, the specific mortality rate (M_0), and maximum specific growth rate of N_2-fixers (μ'_{NF}) and non-fixers (μ'_O) were set at 73, 87.6 and 91.25 yr^{-1}, respectively, and half saturation constant for P and N uptake were also similar to Tyrell's (K_P=0.03 mmol P m^{-3} and K_N=0.05 mmol N m^{-3}). However, the N:P ratios of N_2-fixers (R^{NF}_{org}) and non-fixers (R^{O}_{org}) were not set to equivalent values. Observations show that this ratio can be extremely variable both within and among species (Quigg et al., 2003; Arrigo, 2005). The N:P ratio of N_2-fixers tends to be higher than that of non-fixers (review in White et al., 2006). In our standard simulation, we set R^{NF}_{org} equal to 33 (averaged from Hutchins et al., 2007), while R^{O}_{org} was kept equal to the Redfield ratio of N:P=16. The sensitivity of the model to phytoplankton N:P stoichiometry is addressed later.

The specific mortality rate of zooplankton, M_1, was set at 20 yr^{-1}. This estimation was based on the average value of the zooplankton mortality from the global study of zooplankton mortality (Hirst and Kiørboe, 2002). We also fixed the N:P ratio of

BGD
7, 111–164, 2010

zooplankton (R^{Z}_{org}) at 25, which represents an average for different marine zooplankton (e.g. Le Borgne, 1982; Ikeda and Mitchell, 1982). The fraction of phytoplankton natural mortality associated with predation by herbivores (ε_0) was constrained from global scale assessments of micro- and mesozooplankton grazing (Calbet, 2001; Calbet and Landry, 2004) that suggest that zooplankton consume about 70–80% of the ocean primary production. A value of 80% was chosen here. This critical parameter will be discussed in more detail later in the paper.

As mentioned above, the assimilation efficiency for N and P by herbivores (β^{N} and β^{P}) were not explicitly considered in Sterner's model. Here we included these parameters because sinking faecal pellets can be a significant component of export to the deep ocean. Nitrogen assimilation coefficients for the copepods *Calanus hyperboreus* (Daly, 1997) and *Calanus pacificus* (Landry et al., 1984) are in the ranges 0.73–0.99. Similarly, the study conducted by Vincent et al. (2007) on *Acartia discaudata*, reported an N assimilation efficiency of 87%. In the model, a total of 56.5% of gross intake was released as either NH_4^+ or DON. The resulting N accumulation efficiency (a_N) was 35%, and the GGE was 30%. For P, the range of assimilation coefficients for copepods is 0.4–0.77 (Butler et al., 1970; Corner et al., 1972) and 0.54–0.82 for cladocerans (Peters and Rigler, 1973; Hessen and Andersen, 1990). A compilation of all these values suggests that N and P assimilation efficiencies are in the ranges 0.76–0.99 and 0.4–0.82, respectively. In the standard simulation, we assigned a slightly higher assimilation efficiency for N (β^{N}=69%) than for P (β^{P}=80%) following Anderson et al. (2005).

The maximal accumulation efficiency of either N or P (L_m) could be derived from Eq. (5) using published values of GGE and the assimilation efficiency. Straile (1997) compiled GGE estimates for several taxonomic groups (nano- or microflagellates, dinoflagellates, ciliates, rotifers, cladocerans, and copepods), and found a mean and median of ~20–30%, with maximal values of ~70%. Using an assimilation efficiency of ~70–80%, we thus derived L_m=GGE/β, 0.88–1.00. In the model, we tested different values for L_m (0.75 in the base run, and 0.5 and 0.9 in the sensitivity analyses).

Finally, knowledge about the fraction of N and P remineralised or excreted in the surface layer ($\overline{SR}$) or in the deep ocean ($\overline{DR}$) was essential. The vertical partitioning of remineralisation depended on two parameters, the specific remineralisation rate of detritus and the sinking velocity of particles. In a two box model, we derived estimates of $\overline{SR}$ and $\overline{DR}$ using the following relationships:

$$\overline{SR} = \frac{1}{H} \int_{z=0}^{z=H} \left(1 - e^{\left(-\tau \frac{(H-z)}{V}\right)}\right) p(z) dz \quad (11)$$

and

$$\overline{DR} = 1 - \overline{SR} - SF \quad (12)$$

In this equation, H is the depth of the surface layer, τ is the specific remineralisation rate of detritus (d^{-1}) and V is their sinking velocity ($m\,d^{-1}$), SF is the fraction of organic matter buried in the sediments, and $p(z)$ is a probability distribution for particles in the water column. For simplicity, we assumed that detritus was homogeneously distributed between $z = 0$ and $z = H$. Integration of Eq. (11) between $z = 0$ and $z = H$ yields:

$$\overline{SR} = 1 - \left(1 - e^{\frac{-\tau H}{V}}\right) \frac{V}{\tau H}. \quad (13)$$

An estimate of $\overline{SR}$ required knowledge of the time scale of remineralisation, and of the sinking velocity of detritus. Two studies in temperate and polar systems have reported specific organic matter degradation rates that range from $0.003\,d^{-1}$ to $0.44\,d^{-1}$ and average $0.08 \pm 0.01\,d^{-1}$, with no clear dependence on temperature (Panagiotopoulos et al., 2002; Lønborg et al., 2009). In our model, we used a value of $\tau = 0.1\,d^{-1}$. Sinking velocities depend on the nature of the particles, ranging from $<1\,m\,d^{-1}$ for single phytoplankton cells (Smayda, 1970) to $>700\,m\,d^{-1}$ for aggregates or faecal pellets (Uye and Kaname, 1994; Fischer and Karaka, 2009). In the standard simulation, we set V=2.5 $m\,d^{-1}$, which gave an $\overline{SR}$=0.95, as in Tyrrell's model. The proportion of organic

N and P which escaped remineralisation (SF) was set to 0.3% (Sarmiento and Gruber, 2006), so that $\overline{DR}$=1-(0.95+0.003)=0.047. Finally, excretion of dissolved nutrients from zooplankton was apportioned between the surface layer (SE_1=90% in the base run) and the deep layer (DE_1=10%).

3 Results

3.1 Analytical solutions

Steady state solutions for the model were calculated to provide insights on the processes and parameters which drive the behaviour of the model. These steady solutions were calculated by setting the solution of differential equations to 0.

We used Eqs. (7) and (9) ($dP_S/dt + dP_D/dt$=0), and Eqs. (8) and (10) ($dN_S/dt + dN_D/dt$=0) for a system of two equations with two unknowns, NF^* and O^* (mmol m^{-3}). We thus obtained,

$$NF^* = \frac{1}{M_0 SD}\left[\frac{RPR^O_{org}\left\{SF+DN-SF\beta_1^N\varepsilon_0\left(1-a_N^O\right)\right\}}{\left\{SF\left(1-\beta_1^P\varepsilon_0(1-a_P^O)\right)\right\}} - (AN+RN)\right] \cdot \frac{1}{\left\{1+SF\beta_1^N\varepsilon_0\left(a_N^O-a_N^{NF}\right)\right\}} \quad (14)$$

and

$$O^* = \frac{1}{M_0 SD}\left[\frac{RPR^O_{org}\left\{1-SF-DN+SF\beta_1^N\varepsilon_0\left(1-a_N^{NF}\right)\right\}}{\left\{SF\left(1-\beta_1^P\varepsilon_0(1-a_P^O)\right)\right\}} + (AN+RN)\right] \cdot \frac{1}{\left\{1+SF\beta_1^N\varepsilon_0\left(a_N^O-a_N^{NF}\right)\right\}} \quad (15)$$

As in Tyrrell's (1999) model, both phytoplankton types were primarily limited by the rate of supply and loss of the ultimate limiting nutrient, P. Conversely, the supply of

BGD
7, 111–164, 2010

N from either the atmosphere or rivers had a positive effect on non-fixers (O^*) and a negative one on N_2-fixers (NF^*). In other words, external N inputs to the ocean drove the competition between N_2-fixers and non-fixers.

In our model, the biomass of NF^* and O^* was also controlled by the assimilation of N and P and by the accumulation efficiencies of N and P in herbivores. High assimilation efficiency and low accumulation efficiency of P (β_1^P and a_P^O) favoured both NF^* and O^*. Conversely, high assimilation efficiency and low accumulation efficiency of N had a negative feedback on NF^* and a positive feedback on O^*.

Combining Eqs. (14) and (15) gave the total phytoplankton biomass:

$$(NF^* + O^*) = \frac{1}{M_0 SD}\left[\frac{RP R_{org}^O}{\left\{SF\left(1-\beta_1^P \varepsilon_0 (1-a_P^O)\right)\right\}}\right] \quad (16)$$

Summing Eqs. (14) and (15) cancelled out the role of nitrogen delivery to the ocean and its internal recycling efficiency, so that total phytoplankton biomass ($NF^* + O^*$) was only correlated to the delivery of phosphorus (RP), the N:P stoichiometry of non-fixers (R_{org}^O), burial efficiency (SF), the proportion of primary production channelled towards herbivores (ε_0), and the assimilation and accumulation efficiencies of P (β_1^P and a_P^O). The result of all this was that a high predation rate on a phytoplankton pool that was P-rich compared to the herbivores' requirement resulted in a higher release of P in the dissolved phase which then increased oceanic primary production (see numerical results).

The steady state solution for herbivore biomass (mmol N m^{-3}) was given by:

$$H_1^* = \frac{\left\{\beta_1^N \varepsilon_0 M_0 SD\left(a_N^{NF} NF^* + a_N^O O^*\right)\right\}}{M_1 (SD + DD)}. \quad (17a)$$

Combining Eqs. (14), (15) and (17a) yielded,

$$H_1^* = \frac{\left\{\beta_1^N \varepsilon_0 \left(\frac{RP R_{org}^O \left(a_N^O - \left(SF + DN - SF\beta_1^N \varepsilon_0\right)\left(a_N^O - a_N^{NF}\right)\right)}{\left\{SF\left(1-\beta_1^P \varepsilon_0 (1-a_P^O)\right)\right\}\left\{1+SF\beta_1^N \varepsilon_0 \left(a_N^O - a_N^{NF}\right)\right\}} + \frac{(AN+RN)\left(a_N^O - a_N^{NF}\right)}{\left\{1+SF\beta_1^N \varepsilon_0 \left(a_N^O - a_N^{NF}\right)\right\}} \right)\right\}}{M_1(SD+DD)}. \quad (17b)$$

As expected, the herbivore biomass (in term of units of N) was controlled by the supply of the ultimate limiting nutrient to the ocean (P) and the N:P ratio of phytoplankton. The influence of the supply of P and of the N:P ratio of phytoplankton was however modulated by the assimilation and accumulation efficiencies of N. Unlike for the total phytoplankton biomass, the supply of N, the proximate limiting nutrient of primary production (Tyrrell, 1999), exerted a control on herbivore biomass. Therefore, in the model, both N and P limitation of primary production traveled up the food chain up to herbivores. It should be noted that if $a_N^O = a_N^{NF} = a_N$ (corresponding to the case where $R_{org}^O = R_{org}^{NF}$), the supply of N to the ocean cancelled out from Eq. (17b). The steady state equation then became,

$$H_1^* = \frac{\beta_1^N \varepsilon_0 RP R_{org}^O a_N}{M_1(SD+DD)\left\{SF\left(1-\beta_1^P \varepsilon_0 (1-a_P^O)\right)\right\}}. \quad (17c)$$

Two cases then needed to be considered. If $R_{org}^O \beta_1^N / \beta_1^P < R_{org}^Z$, then N was the element limiting herbivore growth, $a_N = L_m$, and herbivore biomass was positively correlated to R_{org}^O (see model description). Or, if $R_{org}^O \beta_1^N / \beta_1^P > R_{org}^Z$, then P was the limiting element, $a_N = L_m R_{org}^Z / R_{org}^O$, so that R_{org}^O cancelled out from Eq. (17c),

and herbivore biomass (in term of N unit) reached a plateau given by

$$H_1^* = \frac{\beta_1^N \varepsilon_0 RP L_m R_{org}^Z}{M_1(SD+DD)\left\{SF\left(1-\beta_1^P \varepsilon_0 (1-a_P^O)\right)\right\}}. \quad (17d)$$

In this case, herbivore biomass remained constant unless the supply of P to the ocean increased. This general pattern also held when $a_N^O \neq a_N^{NF}$ (see model sensitivity analysis).

The steady state solutions for nutrients concentrations (mmol m^{-3}) were,

$$P_S^* = \frac{M_0 K_P}{\mu'_{NF} - M_0}, \quad (18)$$

$$N_S^* = \frac{M_0 K_N}{\mu'_O - M_0}, \quad (19)$$

and

$$N_D^* = N_S^* + \frac{M_0 SD}{K}\left\{O^* \delta_N^O + NF^* \delta_P^{NF}\right\} \quad (20)$$

with

$\delta_N^O = (1-\varepsilon_0)(DR_0 - 0.25DN) + \varepsilon_0(DR_1 - 0.25DN) + \beta_1^N \varepsilon_0 \left(1 - a_N^O\right)(DE_1 - DR_1)$, and

$\delta_N^{NF} = (1-\varepsilon_0)(DR_0 - 0.25DN) + \varepsilon_0(DR_1 - 0.25DN) + \beta_1^N \varepsilon_0 \left(1 - a_N^{NF}\right)(DE_1 - DR_1)$, and

$$P_D^* = P_S^* + \frac{M_0 SD}{K}\left\{\frac{O^* \delta_P^O}{R_{org}^O} + \frac{NF^* \delta_P^{NF}}{R_{org}^{NF}}\right\} \quad (21)$$

with

$$\delta_P^O = (1-\varepsilon_0)DR_0 + \varepsilon_0 DR_1 + \beta_1^P \varepsilon_0 \left(1 - a_P^O\right)(DE_1 - DR_1),$$

BGD
7, 111–164, 2010

and

$$\delta_{\mathrm{P}}^{\mathrm{NF}} = (1-\varepsilon_0)\mathrm{DR}_0 + \varepsilon_0 \mathrm{DR}_1 + \beta_1^{\mathrm{P}} \varepsilon_0 \left(1 - a_{\mathrm{P}}^{\mathrm{NF}}\right)(\mathrm{DE}_1 - \mathrm{DR}_1).$$

The surface concentrations of both nutrients depended exclusively on the maximum growth rate (μ'_{NF} or μ'_{O}) and the loss term (M_0) for phytoplankton (Tyrrell, 1999). The loss term increased the availability of both nutrients in the surface layer and consequently, provided nutrients for the growth of phytoplankton. Deep concentrations of both nutrients, on the other hand, depended on nutrient supply, nutrient remineralisation processes, and the rate of mixing between the two ocean reservoirs. The origin detritus (phytoplankton, faecal pellets and zooplankton carcasses), together with the nutrient assimilation and accumulation efficiencies of herbivores also worked to control deep nutrient concentrations through the parameters DR_0, DR_1, DE_1, β_1^i and a_i^i.

Total primary production (TPP*, Gt C yr^{-1}) at steady state was deduced from Eq. (16):

$$\mathrm{TPP}^* = \left\{ \frac{\mathrm{RP}R_{\mathrm{org}}^{\mathrm{O}}}{\left\{\mathrm{SF}\left(1 - \beta_1^{\mathrm{P}} \varepsilon_0 (1 - a_{\mathrm{P}}^{\mathrm{O}})\right)\right\}} \right\} \cdot \frac{106}{16} \cdot 12 \cdot \frac{362}{1000} \tag{22}$$

As with Eq. (16), TPP* was primarily controlled by the supply of P to the ocean, as described in Tyrrell (1999), but it was also controlled by recycling through the herbivore parameters. A greater proportion of primary production channelled towards herbivores, together with high assimilation and low accumulation efficiencies for P, increased TPP*. Note that TPP* was converted to Gt C yr^{-1} for the purpose of comparing model output with observations (see Sect. 3.2). In these cases, the standard Redfield C:N ratio of 106:16 was assumed.

Secondary primary production (SPP*, Tmol N yr^{-1}) could also be derived from

$$\mathrm{SPP}^* = \mathrm{SD} \cdot \left\{ \beta_1^{\mathrm{N}} \varepsilon_0 M_0 \left(a_{\mathrm{N}}^{\mathrm{NF}} \mathrm{NF}^* + a_{\mathrm{N}}^{\mathrm{O}} \mathrm{O}^* \right) \right\} \cdot \frac{362}{1000}. \tag{23}$$

Fluxes of various materials at steady state could also be derived (Tmol N yr^{-1}), namely

$$\text{Excretion of nitrogen} = (\text{SD} + \text{DD}) \cdot \left\{ \beta_1^{\text{N}} \varepsilon_0 M_0 \left((1 - a_{\text{N}}^{\text{NF}}) \text{NF}^* + (1 - a_{\text{N}}^{\text{O}}) \text{O}^* \right) \right\} \cdot \frac{362}{1000}, \quad (24)$$

$$\text{Fecal pellet production} = (\text{SD} + \text{DD}) \cdot \left\{ (1 - \beta_1^{\text{N}}) \varepsilon_0 M_0 (\text{NF}^* + \text{O}^*) \right\} \cdot \frac{362}{1000}, \quad (25)$$

and

$$\text{Herbivore mortality} = (\text{SD} + \text{DD}) \cdot M_1 \text{H}_1 \cdot \frac{362}{1000}. \quad (26)$$

3.2 Numerical solutions and model assessment

Numerical solutions were derived by substituting the parameter values (Table 1) into the analytical solutions calculated in Sect. 3.1. These numerical solutions and comparisons to published values are listed in Table 2.

The predicted total phytoplankton biomass (8.5 Tmol N) fell within the literature range (7.5–10.7 Tmol N: Gasol et al., 1997; Tyrrell, 1999), and most of it (99%) was accounted for by non-fixers. Total zooplankton biomass (12.9 Tmol N) was also roughly consistent with the observed range of 8.1 ± 1.9 Tmol N for oceanic systems (Gasol et al., 1997; using a C:N ratio of 5.0 for the conversion). In the meta-analysis of Gasol et al. (1997), protozooplankton accounted for 3.0 ± 0.7 Tmol N and mesozooplankton for 5.1 ± 1.2 Tmol N. This contribution of mesozooplankton is similar to the estimate of Hernandez-León and Ikeda (2005), who gave an estimate of 4.4 ± 0.4 Tmol N.

Our model's prediction for nutrient concentrations was compared to real ocean values using the NOAA-NODC-WOA05 database (Garcia et al., 2006). Matching the scale of integration to the model resolution, we calculated the observed nutrient concentrations in each reservoir. Surface concentrations for both nutrients are lower than given in the literature. This is mainly due to the rough division between the surface (500 m)

and the deep layer (>500 m), as previously noted by Yool and Tyrrell (2003). The predicted N:P ratio in the surface layer ($N^*_S : P^*_S$=13.4) is slightly higher than observed (N:P=12.5), but still N-deficient compared to the canonical Redfield ratio of N:P=16.

Unlike surface nutrients concentrations, deep concentrations of both nutrients were close to the literature value. For the default parameter values listed in Table 1, however, the model converged on a numerical solution in which the deep N:P ratio is lower ($N^*_D : P^*_D$=12.2) than the observed average ($N^*_D : P^*_D$=14.3). From Eqs. (20) and (21), it appears that the deep N:P ratio was controlled primarily by the parameters associated with herbivores, i.e. the assimilation and accumulation efficiencies of N and P (β^N_1, β^P_1, and a^j_i), the fraction of zooplankton excretion which occurred in the deep ocean (DE_1), and the fraction of detritus produced by herbivores which was remineralised in the deep reservoir (DR_1). The sensitivity of the model predictions to these parameters is explored later in Sect. 3.3.

The predicted total primary production, 48.97 Gt C yr^{-1}, falls comfortably within the range of literature values. Global estimates of primary production from satellite radiometer data suggest that 36–61 Gt C are fixed each year by oceanic microalgae (Longhurst, 1995; Antoine et al., 1996; Dunne et al., 2007).

Our model estimated the denitrification of 128 Tg N yr^{-1}, a value which falls into the upper range of recent estimates of denitrification process in water column. Current estimates differ quite significantly, ranging from 65 ± 20 Tg N yr^{-1} (Gruber, 2004) to 116–150 Tg N yr^{-1} (Codispoti et al., 2001; Galloway et al., 2004).

Our model exported 2.45 Gt C yr^{-1} (0.43 Gt N yr^{-1}), or 5.2% of TPP*, to depths deeper than 500 m. This sits at the lower end estimates from the literature (3–25% TPP*) (Schlesinger, 1977; Tyrrell, 1999; Dunne et al., 2007). In our model, most of the export was related to herbivores (0.34 Gt N yr^{-1}) through the production of faecal pellets (0.10 Gt N yr^{-1}) and carcasses (0.13 Gt N yr^{-1}) at depth. Part of the export was also accounted for by excretion below 500 m (0.11 Gt N yr^{-1}).

The predicted total excretion of N (1.2 Gt N yr^{-1}) is at the lower range of global estimates of ammonia excretion by mesozooplankton (1.18–2.38 Gt N yr^{-1},

Hérnandez-León et al., 2008). In addition, it should be note that global estimates of excretion in the ocean would be even higher if microzooplankton excretion was accounted for in observations and if the release of urea and dissolved organic nitrogen (DON) were also considered. Although urea and DON excretion are generally considered to be lower compared to NH_4^+ excretion (Bidigare, 1983), Steinberg and Saba (2008) found that their contribution to total excretion of N varies from 7% to 53% depending on the variety of planktonic crustacean. Excretion of an even greater proportion of N as DON have been reported in *Acartia tonsa*, for example (62–89%, Miller and Glibert, 1998).

In the model, herbivores' excretion depended on the N and P assimilation and accumulation efficiencies. The predicted zooplankton GGE for N (GGE_N) and P (GGE_P) were 52% and 33%, respectively, when zooplankton fed on non-fixers (R^O_{org}= 16). Conversely, when zooplankton fed on N_2 fixers (R^{NF}_{org}=33), GGE_N=45% and GGE_P=60%. Given that the N:P ratio of herbivores was greater than that of non-fixers (owing to the fact that the biomass of non-fixers was considered to be dominant), zooplankton tended to accumulate N more efficiently than P, which resulted in the release of products with a low N:P ratio. DeMott et al. (1998) showed that *Daphnia magna* have a lower GGE when fed on *Scenedemus* with a high P content than when fed on *Scenedemus* having low P content (GGE_P=7% and 50% respectively). A study conducted by Vincent et al. (2007) on *Acartia discaudata* reported a GGE_N of 30%, a value lower than estimated by our model, but the N:P ratio of the algal food was not documented in Vincent et al. study.

It should be pointed out that our modelling assessment was intended to show that our model produces a reasonable fit to the main features of ocean N and P cycling. We have not intended to make a perfect fit with observations as it would be unrealistic to do so with a 2-box model. Rather, our study was conceived to explore the impact of the higher trophic level on N and P cycling at the ocean level as a whole.

3.3 Sensitivity analyses

The main objective of the sensitivity analysis was to determine how ecosystem functions and nutrients inventories respond when (1) the nitrogen to phosphorus ratio (N:P) in phytoplankton varies and when (2) most of primary production is channelled towards herbivores. Attention has also been paid to variations in herbivore parameters.

Herbivore biomass and nutrient GGE – Figure 4a shows how herbivore biomass responds to changes in the N:P ratio of the algal pool. Here we considered only the N:P ratio in phytoplankton that do not fix N_2 because variations of the N:P ratio in N_2-fixers had a smaller impact on model solutions (results not shown). This partly resulted from the low contribution of N_2-fixers to total phytoplankton biomass (~1%, see Tyrrell, 1999). As predicted by Eq. (17d), herbivore biomass increased until the N:P ratio in the algal pool reached a threshold value above which herbivore biomass remained constant unless the N:P ratio of herbivores decreased (Fig. 4a). This threshold ratio corresponded to the case where $R^{O}_{org} = R^{Z}_{org} \cdot \beta^{P}_{1} / \beta^{N}_{1}$ (see Eq. 4), a condition for which the growth of herbivores shifted from N to P limitation. Below this threshold ratio, the excess of P in the phytoplankton pool compared to the herbivore requirement was excreted at a N:P ratio lower than that of phytoplankton (Fig. 4b). In parallel, GGE_P was lower than its maximal value, while, on the other hand, GGE_N was maximal (Fig. 4c). Conversely, above this threshold ratio, phytoplankton nitrogen content was in excess of the herbivore requirement, the N:P ratio of the excreted products increased (Fig. 4b), and GGE_P is maximal while GGE_N decreased exponentially (Fig. 4c).

Phytoplankton biomass and production – Shifts in the accumulation efficiency of N and P maintained the condition of strict homeostasis in the N:P stoichiometry of herbivores, as predicted by Sterner's model (1990). This homeostatic regulation of the elemental composition of herbivores had an impact on the production rates of both N_2-fixers and non-fixers. When the N:P ratio in the algal pool was lower than that of herbivores, the excess P released to seawater favoured the growth of N_2-fixers (which were phosphorus-limited). As a consequence, N_2-fixation increased compared to the

BGD
7, 111–164, 2010

case where herbivores were not considered (Fig. 5a, b). This effect was more pronounced when the difference between the N:P ratio in phytoplankton and herbivores was higher, and/or when the maximal accumulation efficiency ($L_m = a_P$) of phosphorus was lower (Fig. 5a, b).

Figure 5 also shows that the N:P ratio in the algal pool that determined whether N_2 fixation would occur $\left(\left[R^O_{org}\right]_{fix}\right)$ decreased when herbivores were included in the model. This ratio was derived from the steady state solution for N_2-fixers (Eq. 14), and satisfied the following condition:

$$\left[R^O_{org}\right]_{fix} > \frac{(AN+RN)SF\left(1-\beta_1^P\varepsilon_0\right)R^Z_{org}}{RPR^Z_{org}\left\{SF+DN-SF\beta_1^N\varepsilon_0(1-L_m)\right\}-(AN+RN)SF\beta_1^P\varepsilon_0 L_m} \quad (27)$$

Using the default parameters values listed in Table 1, $\left[R^O_{org}\right]_{fix}$ varied from 11.250 without herbivores to 5.536 when herbivores are included in the model. When $R^Z_{org} \to +\infty$, it was found that $\left[R^O_{org}\right]_{fix} \to 4.145$. Conversely, when R^Z_{org} decreased below 16:1, $\left[R^O_{org}\right]_{fix}$ increased exponentially, and became undefined when R^Z_{org} is lower than ~5.5.

The greater fixation of N_2 when herbivores fed on a P-rich algal pool resulted in an input of new N into the surface of the ocean. This new N was eventually available for the N-limited non-fixers (O^*), so that their growth also benefited indirectly from the release of P by herbivores (Fig. 5c, d).

Overall, total primary production (TPP*) increased when herbivores were explicitly considered (Fig. 6). From the steady state solution for TPP* (Eq. 16), the effect of herbivores on TPP* was driven by the term $SF\left(1-\varepsilon_0\beta_1^P\left(1-a_P^O\right)\right)$. All other things being equal, the increase in TPP* was minimal when the accumulation efficiency of P was maximal ($a_P^O = L_m$). This is illustrated on Fig. 6a, b (and also on Fig. 5) by the "straight line" just above the model solution obtained without herbivores

(which corresponds to Tyrell's model). All the model solutions converged towards this straight line when $R^{O}_{org} \geq R^{Z}_{org} \cdot \beta^{P}_{1} / \beta^{N}_{1}$, i.e. when P became the limiting nutrient for herbivore growth (Fig. 4c, d).

Nutrient concentrations and the deep N:P *ratio* – Figure 7 shows the steady state solutions for nutrient concentrations plotted against the N:P ratio of the algal pool. Surface nutrient concentrations were unaffected by variations of the N:P ratio in the algal pool, as expected from the steady state solutions (Eqs. 18 and 19). Deep nutrient concentrations, on the other hand, were affected by variations of the N:P ratio in non-fixers, and by the herbivore parameters (Eqs. 20 and 21). When the N:P ratio in the algal pool increased, the deep N concentration increased and the deep P concentration decreased nonlinearly until $R^{O}_{org} \geq R^{Z}_{org} \cdot \beta^{P}_{1} / \beta^{N}_{1}$.

Using the default parameter set listed in Table 1, this threshold ratio was equal to 28.99. Above 28.99, deep N concentrations increased linearly, while deep P concentrations remained constant. The relative importance of each parameter driving the deep N:P ratio was evaluated using a sensitivity index (SI), calculated as follows,

$$\mathrm{SI} = \frac{1}{n} \sum_{R^{O}_{org}=1}^{R^{O}_{org}=n} \frac{\sqrt{\left(X^{R^{O}_{org}}_{std} + X^{R^{O}_{org}}_{-50\%} \right)^{2}}}{X^{R^{O}_{org}}_{std}} \tag{28}$$

In this Eq., $X^{R^{O}_{org}}_{std}$ is the model solution for a variable X (deep nutrient concentrations and N:P ratio) using the default parameter set listed in Table 1 and the variable N:P ratio in non-fixers (R^{O}_{org}). $X^{R^{O}_{org}}_{-50\%}$ is the model solution for the same variable when a model parameter has been decreased by 50%. We tested values for R^{O}_{org} from R^{O}_{org}=1 to R^{O}_{org}=50. The results (Table 3) show that deep nutrient concentrations were primarily controlled by the mixing rate (K) and herbivores' parameters, notably L_m, DR_1, ε_0, β^{P}_{1}, and SE_1.

Deep nutrient concentrations were less sensitive to the other parameters, DR_0, R^Z_{org}, DN and β^N_1.

The predicted deep N:P ratio was mainly controlled by two parameters: SE_1 and DR_1. Figure 8 illustrates the sensitivity of the predicted deep ocean N:P ratio to variations of both the N:P ratio of non-fixers and SE_1. In contrast to Tyrrell's original model, changes in the deep nutrient N:P ratio were nonlinearly related to the phytoplankton N:P ratio. Higher SE_1 (i.e. a lower proportion of excretion occurring in the deep ocean) tended to reduce changes in deep nutrient N:P ratios when phytoplankton stoichiometry varied, notably when $R^O_{org} > R^Z_{org} \cdot \beta^P_1 / \beta^N_1$. In this case, deviations from Redfield stoichiometry in phytoplankton were partly absorbed in the surface of the ocean through the excretion of the excess of N. Conversely, a lower SE_1 amplified the increase in the deep nutrient N:P ratio when R^O_{org} was higher than $R^Z_{org} \cdot \beta^P_1 \beta^N_1$ and reduced it when R^O_{org} was lower.

Figure 9 shows the estimated deep ocean N* for different N:P ratios in herbivores (R^Z_{org}) and for different values of SE_1. Gruber and Sarmiento (1997) introduced this N* parameter to derive estimates of N_2-fixation and denitrification in the ocean, defining it as:

$$N^* = [NO_3^-] - 16[PO_4^{3-}] + 2.9 \quad \text{mmol N m}^{-3}. \tag{29}$$

As shown on Fig. 9, the actions of herbivores may alter the deep ocean N*. Low R^Z_{org} ($R^Z_{org} < R^O_{org} \cdot \beta^P_1 / \beta^N_1$ or <13.8) and high SE_1 ($SE_1 \geq 0.95$) induced positive N* values. Strong negative N* values were predicted when R^Z_{org} (>13.8) increased and SE_1 decreased ($SE_1 \leq 0.95$). When 100% excretion occurred in the surface and R^Z_{org} was high, N* values became positive. This implies that differential recycling of N and P by herbivores in the surface of the ocean can induce a N deficit (negative N*) or an excess of N in the deeper layers that do not result from either denitrification or N_2-fixation.

4 Discussion

The main question addressed in this study was to what extent does CNR drive oceanic primary production and the distribution of N and P in the global ocean? To answer this question, we used a model built upon foundations provided by Tyrrell (1999) and Sterner (1990). The model was kept admittedly simple in term of the N and P metabolism of phytoplankton and herbivores. Regarding herbivores, however, Sterner's approach has been proven robust in estimating observed patterns of CNR (Sterner and Elser, 2002).

Our combination of these two models has shown that marine herbivores may exert a control on global primary productivity through the resupply and the stoichiometry of N and P in the ocean.

In the model, P remained the ultimate limiting nutrient of marine productivity, as in Tyrell's (1999) original model. When herbivores were included in the model, however, variations of marine primary productivity resulted not only from variations in the inputs of P from rivers (Tyrrell, 1999), but also from CNR. Levels of global primary production were higher particularly when herbivores had higher N:P ratios than phytoplankton (Fig. 6). This higher primary production was triggered by a low N:P resupply ratio from herbivores (Fig. 4b), which in turn favoured the P-limited N_2-fixation (Fig. 5a, b). Eventually, the N-limited non-fixers benefited from the input of this "new N" fuelled by N_2-fixation (Fig. 5c, d).

This influence of CNR on N_2-fixation has been demonstrated in lakes, with reduced N_2-fixation when herbivores were composed of *Daphnia pulex*, a species with low whole-body N:P ratios, while N_2-fixation was higher with herbivores having higher N:P ratios (MacKay and Elser, 1998). In the ocean, evidences for P-limitation of N_2-fixation and for low N:P resupply ratios from migrating zooplankton have been also documented in the Pacific subtropical gyres (Moutin et al., 2005; Hannides et al., 2009). Additionally, it has been shown that marine species of microzooplankton have usually a low N:P resupply ratio, in the range 2:1 to 8:1 (Dolan, 1997).

BGD
7, 111–164, 2010

Our results, therefore, support the idea that in the oceanic P-limited systems, grazing by herbivores, notably microzooplankton, may alleviate P-limitation of marine productivity.

The model has also revealed that CNR can influence the N:P ratio in non-fixers that trigger N_2-fixation ($\left[R^{O}_{org}\right]_{fix}$, Eq. (27)). Using a modified version of Tyrrell's (1999) model, Lenton and Klausmeier (2007) found that competitive dynamics between N_2-fixers and non-fixers competitive dynamics set the N:P threshold for N_2-fixation. Here, we found that when the N:P ratio in herbivores (R^{Z}_{org}) increased above Redfield stoichiometry, $\left[R^{O}_{org}\right]_{fix}$ converged towards a constant value of ~4–5, while $\left[R^{O}_{org}\right]_{fix}$ increased sharply when R^{Z}_{org} converged towards a value of ~5–6.

Values for $\left[R^{O}_{org}\right]_{fix}$ of ~4–5 fall in the lower range of observed N:P ratios in phytoplankton (Quigg et al., 2003). These values are, to our knowledge, rarely encountered in natural marine phytoplankton communities. Similarly, a review of the N:P ratio in marine zooplankton has shown that most of these organisms, excepted fish larvae, have a N:P ratio usually higher or close to 16:1 (Table 4). Therefore, our results would suggest that N_2-fixation should be rarely triggered by the N:P ratios of non-fixers in most of the cases encountered in the ocean.

The model has also shown that phytoplankton with higher N:P ratios increased the yield of herbivores until $R^{O}_{org} \geq R^{Z}_{org} \cdot \beta^{P}_{1} / \beta^{N}_{1}$ (Fig. 4), when P became the element limiting herbivore growth. As predicted by Sterner's model, this case favoured herbivores with a low P-requirement (or high N:P ratios; Fig. 4). Such situations have been reported in lakes where zooplankton community assemblages with lower P requirements are correlated with high C:P ratios in the seston (Gulati et al., 1991). In the ocean, P-limitation has been reported in various systems, notably in the oligotrophic gyres (Karl et al., 2001; Moutin et al., 2005).

BGD
7, 111–164, 2010

Such systems would be useful for testing whether or not phytoplankton communities with higher N:P ratios, such as *Synechoccocus* or *Prochlorochoccus* (Bertilsson et al., 2003), also favour zooplankton assemblages with low P requirement in the ocean.

Finally, the model suggested that CNR both drove and buffered the impact of deviations from Redfield stoichiometry in non-fixers on the deep ocean N:P ratio. This influence of CNR was driven by three mechanisms, the importance of herbivory which accounted for 80% of the annual primary production in the model, the homeostatic regulation of herbivore's N:P stoichiometry, and the resulting excretion of N and P in various proportions.

When most of the excretion occurred in the surface of the ocean, CNR reduced the impact of variations of the N:P ratio in non-fixers on the deep N:P ratio (Fig. 8). Then, The deep N:P ratio tended to mimic the N:P ratio of herbivores rather than that of phytoplankton. Additionally, N deficit (N*<0) or N excess (N*>0) can result not only from shifts in the balance between N_2-fixation and denitrification (Gruber and Sarmiento, 1997), but also from CNR. When R^{Z}_{org} was higher than Refield stoichiometry, this induced N excess in the deep ocean if more than 95% of the excretion occurred in the surface of the ocean (Fig. 9). Conversely, N deficit was found when more that ~5% of the excretion occurred in the deep ocean (Fig. 9).

In other words, if primary production is mainly consumed by non-migrating zooplankton with high N:P ratios, such as microzooplankton, most of the excretion will occur in the surface of the ocean, thereby inducing N excess in the deeper layers (Fig. 9). In this case, estimates of denitrification in the deep ocean from N* calculations could be underestimated. Conversely, migrating herbivores, such as mesozooplankton, will excrete part of the nutrients in the deep layers with a low N:P resupply ratio. This active transport of nutrients could induce N deficit in the deeper layers (Fig. 9), and a possible overestimation of denitrification.

In the North Pacific gyre, Hannides et al. (2009) have shown that P fluxes to the deeper layers mediated by excretion from migrating zooplankton was a significant component of P cycling in this area. This active downward flux of P was shown to be equal

in magnitude to the P flux mediated by particles sinking, thereby reinforcing P-limitation of marine productivity in the upper layers. Additionally, this P-rich flux mediated by migrating zooplankton may induce apparent N deficit in the deeper layers that would not result from denitrification.

All together, our model results and recent studies in the subtropical gyres suggest that marine herbivores and CNR may be important in driving the stoichiometry of N and P in the deep ocean, and should be included in efforts to understand biogeochemical cycles. Although simple, the proposed parameterisation of the influence of CNR on oceanic N and P cycles is driven by some critical parameters which need further investigations.

(1) Proportion of primary production channelled towards herbivores – A key parameter in the model was the proportion of primary production channelled towards herbivores (set at ε_0=0.8) rather than exported. However, this parameter may vary in space and time. As noted previously, grazing estimates based on dilution experiments have shown that heterotrophic protists consume an average of 67% of the daily phytoplankton growth, with higher proportions found in the open ocean (Calbet and Landry, 2004). This is in line with the idea that, in the ocean, the dynamics of pico- and nanophytoplankton communities are notably controlled by grazing pressure (Sherr and Sherr, 1994, 2002), which eventually results in efficient recycling of nutrients in surface waters (Azam et al., 1983; Legendre and Rassoulzadegan, 1995).

Large microphytoplankton, on the other hand, can more easily escape from grazing. Calbet (2001) found for example that mesozooplankton (200–20 000 µm in size) consume an average of 12% of the annual oceanic primary production. Locally, salps or large krill swarms can consume a significant proportion of the daily primary production on a short time scale. Von Bodungen (1986) found, for example, that krill swarms can consume up to 45% of the daily primary production over a period of 3 weeks in the Brandsfield Strait (Southern Ocean).

The proportion of primary production channelled towards herbivores will thus vary both temporally and spatially, according to the dominance of phytoplankton communities by either small or large organisms. Summing the contribution of protists and mesozooplankton gives an estimate of 79% –87% of the oceanic primary production being exported towards herbivores.

A process, not included in the model, which would also result in an efficient remineralisation of organic matter within the upper ocean, is cell lysis associated with virus infections. Cell lysis rates can be high (up to 87.8 d^{-1}) in the ocean and may account for a significant part of small phytoplankton natural mortality (Marbá et al., 2007). Higher latitudes, coastal areas, or fronts are, conversely, characterised by seasonal blooms dominated by large phytoplankton such as diatoms. Bloom terminations often result in the export and mass sedimentation of large aggregates which contains various particles, including exopolymers like mucus, transparent exopolymer particles (TEP), phytoplankton cells, detritus, faecal pellets, minerals and mucus (Thornton, 2002).

(2) Release of unassimilated nutrients between soluble (excreted) and particulate forms (egested) and proportion of excretion occuring in the surface of the ocean – The release of unassimilated nutrients between soluble (excreted) and particulate (egested) forms together with the proportion of excreted to egested nutrients remineralised in the surface of the ocean are also critical model parameters.

To our knowledge, few things are known about the proportion of the excretion occurring in the surface of the ocean. A significant proportion of excretion is likely accounted for by small organisms (nano- and microzooplankton) which have high turnover rates. These organisms do not perform large vertical migrations, and should excrete N or P mostly in the surface of the ocean. Also, they produce minipellets which are mostly remineralised in the surface (Gowing and Silver, 1985; Nöthig and Von Bodungen, 1989; González, 1993). A study on microzooplankton grazing in the Southern Ocean suggested, for example, that during winter, the efficiency of the biological carbon pump is reduced when a greater proportion of the photosynthetically fixed carbon is passed to the microzooplankton compared to summer when the larger cells

dominate phytoplankton biomass and the bulk of the photosynthetically fixed carbon are consumed by meso- and macrozooplankton (Froneman and Perissinotto, 1996).

Unlike nano- and microzooplankton, large organisms like copepods and other large crustaceans can vertical migrate on short time scales. Various studies show that excretion by these organisms below the euphotic zone can account for a significant part of the biological pump and the vertical flux of nutrients in a variety of open-ocean environments (Longhurst et al., 1990; Dam et al., 1995; Le Borgne and Rodier, 1997; Steinberg et al., 2000; Al-Mutairi and Landry, 2001; Steinberg et al., 2002). Hernandez-León and Ikeda (2005) also reported that ~10-15% of mesozooplankton respiration ($13.0 \pm 4.2\,\mathrm{Gt\,C\,yr^{-1}}$) occurs at depths deeper than 500 m. Part of this deep excretion is accounted for by organisms which feed in surface layers and excrete part of their assimilated nutrients in the mesopelagic zone.

If we combine the contribution of protists and mesozooplankton to grazing and global excretion, we can reasonably suggest that ~90% of the excretion occurs at depths shallower than 500 m. This vertical partitioning needs further investigation with regards to its importance in driving the deep nutrient inventories, as illustrated by the model presented herein.

5 Conclusion and perspectives

By linking the two important works of Tyrrell (1999) and Sterner (1990), this study has shed light on the possible role of herbivores in driving N and P cycles in the ocean, following the pathways of N and P from food source, incorporation into herbivorous zooplankton, the resulting metabolic products, and, finally, nutrient inventories. Although simple, the model used here emphasises the need for us to better understand how consumers influence nutrient recycling in the ocean. This study should be extend to higher trophic levels, beyond herbivores. As pointed at by Sterner and Elser (2002), the fate of N and P which are channelled towards herbivores versus carnivores remain poorly constrained.

The model presented here does not discriminate between herbivorous protists and mesozooplankton, the later which are able to feed actively on protists (Gismervik and Andersen, 1997). Also, there is evidence that predation accounts for a significant proportion of natural mortality in small marine invertebrates, up to 70–80% in copepods for example (Hirst and Kiørboe, 2002).

The elemental stoichiometry of marine predators is still poorly documented compared to freshwater organisms and needs further investigations. A study in the Baltic Sea has shown for example that the biomass of pelagic fishes could represent a significant pool of P (Hjerne and Hansson, 2002), thereby influencing nutrient cycling in this system.

In conclusion, the two models used here support the idea that CNR may influence nutrient cycling and inventories at global scale and that this process should be account for in ocean physical-biological models which often assume Redfield stoichiometry throughout the food chain.

Acknowledgements. This research was funded by the EU Marie Curie EST project METAOCEANS (MEST-CT-2005-019678) and supported by CNRS-INSU. The writers would like to thank Christina De La Rocha for constructive comments on the manuscript, and Pascal Rivière, Camille Mazoyer and Coralie Perruche for their help in constructing the model.

The publication of this article is financed by CNRS-INSU.

References

Al-Mutairi, H. and Landry, M. R.: Active export of carbon and nitrogen at Station ALOHA by diel migrant zooplankton, Deep-Sea Res. Pt. II, 48, 2083–2103, 2001.

Anderson, T. R., Hessen, D. O., Dag, O., Elser, J. J., and Urabe, J.: Metabolic stoichiometry and the fate of excess carbon and nutrients in consumers, Am. Nat., 165, 1–15, 2005.

Antoine, D., André, J. M., and Morel, A.: Oceanic primary production 2, Estimation at global scale from satellite (coastal zone color scanner) chlorophyll, Glob. Biogeochem. Cy., 10, 57–69, 1996.

Arrigo, K. R.: Marine microorganisms and global nutrient cycles, Nature, 437, 349–355, 2005.

Azam, F., Fenchel, T., Field, J. G., Gray, J. S., Meyer-Reil, L. A., and Thingstad, F.: The ecological role of water-column microbes in the sea, Mar. Ecol.-Prog. Ser., 10, 257–263, 1983.

Barnes, R. S. K. and Hughes, R. N.: An introduction to marine ecology, 3. Edn., Wiley-Blackwell, 296 pp., 1999.

Beers, J. R.: About microzooplankton, in: Phytoplankton manual. Monographs on oceanographic methodology, edited by: Sournia, A., Unesco Press, Paris, 288–296, 1978.

Bertilsson, S., Berglund, O., Karl, D. M. and Chisolm, S. W.: Elemental composition of marine *Prochlorococcus* and *Synechococcus*: implications for the ecological stoichiometry of the sea, Limnol. Oceanogr., 48, 1721–1731, 2003.

Besiktepe, S. and Dam, H. G.: Coupling of ingestion and defecation as a function of diet in the calanoid copepod *Acartia tonsa*, Mar. Ecol.-Prog. Ser., 229, 151–164, 2002.

Bidigare, R. R.: Nitrogen excretion by marine zooplankton, in: Nitrogen in the marine environment, edited by: Carpenter, E. J. and Capone, D. G., Academic Press, New York, 385–409, 1983.

Broecker, W. S. and Peng, T. H.: Tracers in the sea, Lamont-Doherty Geological Observatory, Palisades, New York, 690 pp., 1982.

Butler, E. I., Corner, E. D. S., and Marshall, S. M.: On the nutrition and metabolism of zooplankton. VII, Seasonal survey of nitrogen and phosphorus excretion by *Calanus* in the Clyde Sea area, J. Mar. Biol. Assoc. UK, 50, 525–560, 1970.

Calbet, A.: Mesozooplankton grazing effect on primary production: A global comparative analysis in marine ecosystems, Limnol. Oceanogr., 46, 1824–1830, 2001.

Calbet, A. and Landry, M.: Phytoplankton growth, microzooplankton grazing, and carbon cycling in marine systems, Limnol. Oceanogr., 49, 51–57, 2004.

Cebrián, J.: Grazing on benthic primary producers, in: Estuarine nutrient cycling: The influence of primary producers, edited by: Nielsen, S. L., Banta, G. T., and Pedersen, M. F., Springer, Netherlands, 153–185, 2004.
Codispoti, L. A., Brandes, J. A., Christensen, J. P., Devol, A. H., Naqvi, S. W. A., Paerl, H. W., and Yoshinari, T.: The oceanic fixed nitrogen and nitrous oxide budgets: Moving targets as we enter the anthropocene?, Sci. Mar., 65, 85–105, 2001.
Compton, J., Mallinson, D., Glenn, C. R., Filippelli, G., Follmi, K., Shields, G., and Zanin, Y.: Variations in the global phosphorus cycle, SEPM Spec. P., 66, 21–34, 2000.
Corner, E. D., Head, R. N., and Kilvington, C. C.: On the nutrition and metabolism of zooplankton: The grazing of Biddulphia cells by *Calanus helgolandicus*, J. Mar. Biol. Assoc. UK, 53, 847–861, 1972.
Corner, E. D. S. and Davies, A. G.: Plankton as a factor in the nitrogen and phosphorus cycles in the sea, Adv. Mar. Biol., 9, 101–204, 1971.
Daly, K.: Flux of particulate matter through copepods in the Northeast water polynya, J. Marine Syst., 10, 319–342, 1997.
Dam, H., Roman, M., and Youngbluth, M.: Downward export of respiratory carbon and dissolved inorganic nitrogen by diel-migrant mesozooplankton at the JGOFS Bermuda time-series station, Deep-Sea Res. Pt. I, 42, 1187–1197, 1995.
DeMott, W. R., Gulati, R. D., and Siewertsen, K.: Effects of phosphorus-deficient diets on the carbon and phosphorus balance of *Daphnia magna*, Limnol. Oceanogr., 43, 1147–1161, 1998.
Dolan, J. R.: Phosphorus and ammonia excretion by planktonic protists, Mar. Geol., 139, 109–122, 1997.
Downing, J. A.: Marine nitrogen: phosphorus stoichiometry and the global N:P cycle, Biogeochemistry, 37, 237–252, 1997.
Duarte, C. M. and Cebrián, J.: The fate of marine autotrophic production, Limnol. Oceanogr., 41, 1758–1766, 1996.
Dugdale, R. C. and Goering, J. J.: Uptake of new and regenerated forms of nitrogen in primary productivity, Limnol. Oceanogr., 12, 196–206, 1967.
Dunne, J. P., Sarmiento, J. L., and Gnanadesikan, A.: A synthesis of global particle export from the surface ocean and cycling through the ocean interior and on the seafloor, Glob. Biogeochem. Cy., 21, GB4006, doi:10.1029/2006gb002907, 2007.
Elser, J. J. and Urabe, J.: The stoichiometry of consumer-driven nutrient recycling: Theory,

observations, and consequences, Ecology, 80, 735–751, 1999.
Fischer, G. and Karakaş, G.: Sinking rates and ballast composition of particles in the Atlantic Ocean: implications for the organic carbon fluxes to the deep ocean, Biogeosciences, 6, 85–102, 2009, http://www.biogeosciences.net/6/85/2009/.
Froneman, P. and Perissinotto, R.: Microzooplankton grazing in the Southern Ocean: Implications for the carbon cycle, Mar. Ecol.-Evol. Persp., 17, 99–115, 1996.
Galloway, J. N., Dentener, F. J., Capone, D. G., Boyer, E. W., Howarth, R. W., Seitzinger, S. P., Asner, G. P., Cleveland, C. C., Green, P. A., Holland, E. A., Karl, D. M., Michaels, A. F., Porter, J. H., Townsend, A. R., and Vöosmarty, C. J.: Nitrogen cycles: Past, present, and future, Biogeochemistry, 70, 153–226, 2004.
Garcia, H. E., Locarnini, R. A., Boyer, T. P., and Antonov, J. I., in: World Ocean Atlas 2005, Nutrients (phosphate, nitrate, silicate), edited by: Levitus, S., NOAA Atlas NESDIS 64, US Government Printing Office, Washington DC, 396 pp., 2006.
Gasol, J. M., del Giorgio, P. A., and Duarte, C. M.: Biomass distribution in marine planktonic communities, Limnol. Oceanogr., 42, 1353–1363, 1997.
Geider, R. J. and La Roche, J.: Redfield revisited: Variability of C:N:P in marine microalgae and its biochemical basis, Eur. J. Phycol., 37, 1–17, 2002.
Gismervik, I.: Stoichiometry of some marine planktonic crustaceans, J. Plankton Res., 19, 279–285, 1997.
Gismervik, I. and Andersen, T.: Switching between herbivory and carnivory by a calanoid copepod: Experimental evidence and food web implications assessed by a model, Mar. Ecol.-Prog. Ser., 157, 247–259, 1997.
González, H. E.: Distribution and abundance of minipellets around the Antarctic peninsula. Implications for protistan feeding behaviour, Mar. Ecol.-Prog. Ser., 90, 223–223, 1993.
Gowing, M. M. and Silver, M. W.: Minipellets: A new and abundant size class of marine fecal pellets, J. Mar. Res., 43, 395–418, 1985.
Gruber, N. and Sarmiento, J. L.: Global patterns of marine nitrogen fixation and denitrification, Glob. Biogeochem. Cy., 11, 235–266, 1997.
Gruber, N.: The dynamics of the marine nitrogen cycle and its influence on atmospheric CO_2 variations, in: The ocean carbon cycle and climate, edited by: Follows, M. and Oguz, T., NATO Science Series, 97–148, 2004.
Gruber, N.: The marine nitrogen cycle: Overview and challenges, in: Nitrogen in the marine en-

vironment, 2. Edn., edited by: Capone, D. G., Bronk, D. A., Mulholland, M. R., and Carpenter, E. J., Academic Press, Boston, MA, 1–50, 2008.
Gruber, N. and Galloway, J. N.: An Earth-system perspective of the global nitrogen cycle, Nature, 451, 293–296, 2008.
Gulati, R. D., Siewertsen, K., and Van Liere, L.: Carbon and phosphorus relationships of zooplankton and its seston food in Loosdrecht lakes, Mem. Ist. Ital. Idrobiol, 48, 279–298, 1991.
Hannides, C. C. S., Landry, M., Benitez-Nelson, C. R., Styles, R. M., Montoya, J. P., and Karl D. M.: Export stoichiometry and migrant-mediated flux of phosphorus in the North Pacific subtropical gyre, Deep-Sea Res. Pt. I, 56, 73–88, 2009.
Hérnandez-León, S. and Ikeda, T.: A global assessment of mesozooplankton respiration in the ocean, J. Plankton Res., 27, 153–158, 2005.
Hérnandez-León, S., Fraga, C., and Ikeda, T.: A global estimation of mesozooplankton ammonium excretion in the open ocean, J. Plankton Res., 30, 577–585, 2008.
Hessen, D. and Andersen, T.: Bacteria as a source of phosphorus for zooplankton, Hydrobiologia, 206, 217–223, 1990.
Hirst, A. G. and Kiørboe, T.: Mortality of marine planktonic copepods: Global rates and patterns, Mar. Ecol.-Prog. Ser., 230, 195–209, 2002.
Hjerne, O. and Hansson, S.: The role of fish and fisheries in Baltic Sea nutrient dynamics, Limnol. Oceanogr., 47, 1023–1032, 2002.
Howarth, R. W.: Nutrient limitation of net primary production in marine ecosystems, Annu. Rev. Ecol. Syst., 19, 89–110, 1988.
Hutchins, D. A., Fu, F. X., Zhang, Y., Warner, M. E., Feng, Y., Portune, K., Bernhardt, P. W., and Mulholland, M. R.: CO_2 control of *Trichodesmium* N_2 fixation, photosynthesis, growth rates, and elemental ratios: Implications for past, present, and future ocean biogeochemistry, Limnol. Oceanogr., 52, 1293–1304, 2007.
Hutchins, D. A. and Fu, F.: Linking the oceanic biogeochemistry of iron and phosphorus with the marine nitrogen cycle, in: Nitrogen in the marine environment, 2. Edn., edited by: Capone, D. G., Bronk, D. A., Mulholland, M. R., and Carpenter, E. J., Elsevier, 1627–1666, 2008.
Iguchi, N. and Ikeda, T.: Metabolism and elemental composition of aggregate and solitary forms of *Salpa thompsoni* (Tunicata: Thaliacea) in waters off the Antarctic Peninsula during austral summer 1999, J. Plankton Res., 26, 1025–1037, 2004.
Ikeda, T. and Mitchell, A. W.: Oxygen uptake, ammonia excretion and phosphate excretion by krill and other antarctic zooplankton in relation to their body size and chemical composition,

Mar. Biol., 71, 283–298, 1982.
Karl, D. M., Björkman, K. M., Dore, J. E., Fujieki, L., Hebel, D. V., Houlihan, T., Letelier, R. M., and Tupas, L. M.: Ecological nitrogen-to-phosphorus stoichiometry at station ALOHA, Deep-Sea Res. Pt. II, 48, 1529–1566, 2001.
Klausmeier, C. A., Litchman, E., and Levin, S. A.: Phytoplankton growth and stoichiometry under multiple nutrient limitation, Limnol. Oceanogr., 49, 1463–1470, 2004.
Landry, M. R., Hassett, R. P., Fagerness, V., Downs, J., and Lorenzen, C. J.: Effect of food acclimation on assimilation efficiency of *Calanus pacificus*, Limnol. Oceanogr., 29, 361–364, 1984.
Landry, M. R. and Calbet, A.: Microzooplankton production in the oceans, ICES J. Mar. Sci., 61, 501–507, 2004.
Le Borgne, R.: Zooplankton production in the Eastern Tropical Atlantic Ocean: Net growth efficiency and P:B in terms of carbon, nitrogen, and phosphorus, Limnol. Oceanogr., 27, 681–698, 1982.
Le Borgne, R. and Rodier, M.: Net zooplankton and the biological pump: a comparison between the oligotrophic and mesotrophic equatorial Pacific, Deep-Sea Res. Pt. II, 44, 2003–2023, 1997.
Legendre, L. and Rassoulzadegan, F.: Plankton and nutrient dynamics in marine waters, Ophelia, 41, 153–172, 1995.
Lenton, T. M. and Klausmeier, C. A.: Biotic stoichiometric controls on the deep ocean N:P ratio, Biogeosciences, 4, 353–367, 2007, http://www.biogeosciences.net/4/353/2007/.
Lønborg, C., Davidson, K., Álvarez-Salgado, X. A., and Miller, A. E. J.: Bioavailability and bacterial degradation rates of dissolved organic matter in a temperate coastal area during an annual cycle, Mar. Chem., 113, 219–226, 2009.
Longhurst, A.: Seasonal cycles of pelagic production and consumption, Prog. Oceanogr., 36, 77–167, 1995.
Longhurst, A. R., Bedo, A. W., Harrison, W. G., Head, E. J. H., and Sameoto, D. D.: Vertical flux of respiratory carbon by oceanic diel migrant biota, Deep-Sea Res., 37, 685–694, 1990.
MacKay, N. A. and Elser, J. J.: Factors potentially preventing trophic cascades: Food quality, invertebrate predation, and their Interaction, Limnol. Oceanogr., 43, 339–347, 1998.
Mackenzie, F. T., Ver, L. M., Sabine, C., Lane, M., and Lerman, A.: C, N, P, S global biogeochemical cycles and modeling of global change, NATO ASI Series I, edited by: Wollast, R.,

Mackenzie, F. T., and Chou, L., Springer-Verlag, New York, 162 pp., 1993.
Marbá, N., Duarte, C. M., and Agustí, S.: Allometric scaling of plant life history, P. Natl. Acad. Sci. USA, 104, 15777–15780, 2007.
Miller, C. A. and Landry, M. R.: Ingestion-independent rates of ammonium excretion by the copepod *Calanus pacificus*, Mar. Biol., 78, 265–270, 1984.
Miller, C. A. and Glibert, P. M.: Nitrogen excretion by the calanoid copepod *Acartia tonsa*: results of mesocosm experiments, J. Plankton Res., 20, 1767–1780, 1998.
Moutin, T., Van Den Broeck, N., Beker, B., Dupouy, C., Rimmelin, P., and Le Bouteiller, A.: Phosphate availability controls *Trichodesmium* spp. biomass in the SW Pacific Ocean, Mar. Ecol.-Prog. Ser., 297, 15–21, 2005.
Nejstgaard, J., Tang, K., Steinke, M., Dutz, J. o., Koski, M., Antajan, E., and Long, J.: Zooplankton grazing on *Phaeocystis*: a quantitative review and future challenges, Biogeochemistry, 83, 147–172, 2007.
Nöthig, E. M. and Von Bodungen, B.: Occurrence and vertical flux of faecal pellets of probably protozoan origin in the southeastern Weddell Sea (Antarctica), Mar. Ecol.-Prog. Ser., 56, 281–289, 1989.
Panagiotopoulos, C., Sempéré, R., Obernosterer, I., Striby, L., Goutx, M., Van Wambeke, F., Gautier, S., and Lafont, R.: Bacterial degradation of large particles in the southern Indian Ocean using in vitro incubation experiments, Org. Geochem., 33, 985–1000, 2002.
Peters, R. H. and Rigler, F. H.: Phosphorus release by *Daphnia*, Limnol. Oceanogr., 18, 821–839, 1973.
Pilati, A. and Vanni, M. J.: Ontogeny, diet shifts, and nutrient stoichiometry in fish, Oikos, 116, 1663–1674, 2007.
Quigg, A., Finkel, Z. V., Irwin, A. J., Rosenthal, Y., Ho, T.-Y., Reinfelder, J. R., Schofield, O., Morel, F. M. M., and Falkowski, P. G.: The evolutionary inheritance of elemental stoichiometry in marine phytoplankton, Nature, 425, 291–294, 2003.
Redfield, A. C.: On the proportions of organic derivations in sea water and their relation to the composition of plankton, edited by: Daniel, R. J., University Press of Liverpool, 176–192, 1934.
Redfield, A. C., Ketchum, B. H., and Richards, F. A.: The influence of organisms on the composition of sea-water, in: The Sea. Vol. 2., edited by: Hill, M. N., Interscience Publishers New York, 26–77, 1963.
Roger, C.: Bioecological sheets on tropical Pacific euphausiids, Office de la Recherche Scien-

tifique et Technique Outre-Mev, 265 pp., 1978.
Ryther, J. H. and Dunstan, W. M.: Nitrogen, phosphorus, and eutrophication in the coastal marine environment, Science, 171, 1008–1013, 1971.
Sarmiento, J. L. and Gruber, N.: Ocean biogeochemical dynamics, Princeton University Press, 526 pp., 2006.
Schlesinger, W. H.: Biogeochemistry – An analysis of global change, Academic Press, 588 pp., 1977.
Sherr, E. B. and Sherr, B. F.: Bacterivory and herbivory: Key roles of phagotrophic protists in pelagic food webs, Microb. Ecol., 28, 223–235, 1994.
Sherr, E. B. and Sherr, B. F.: Significance of predation by protists in aquatic microbial food webs, Antonie van Leeuwenhoek, 81, 293–308, 2002.
Slomp, C. P. and Van Cappellen, P.: The global marine phosphorus cycle: sensitivity to oceanic circulation, Biogeosciences, 4, 155–171, 2007, http://www.biogeosciences.net/4/155/2007/.
Smayda, T. J.: The suspension and sinking of phytoplankton in the sea, Oceanogr. Mar. Biol., 8, 353–414, 1970.
Steinberg, D., Goldthwait, S., and Hansell, D.: Zooplankton vertical migration and the active transport of dissolved organic and inorganic nitrogen in the Sargasso Sea, Deep-Sea Res. Pt. I, 49, 1445–1461, 2002.
Steinberg, D. K., Carlson, C. A., Bates, N. R., Goldthwait, S. A., Madin, L. P., and Michaels, A. F.: Zooplankton vertical migration and the active transport of dissolved organic and inorganic carbon in the Sargasso Sea, Deep-Sea Res. Pt. I, 47, 137–158, 2000.
Steinberg, D. K. and Saba, G. K.: Nitrogen consumption and metabolism in marine zooplankton, in: Nitrogen in the marine environment, 2. Edn., edited by: Capone, D. G., Bronk, D. A., Mulholland, M. R., and Carpenter, E. J., Academic Press, Boston, MA, 1135–1196, 2008.
Sterner, R. W.: The ratio of nitrogen to phosphorus resupplied by herbivores: Zooplankton and the algal competitive arena, Am. Nat., 136, 209–229, 1990.
Sterner, R. W., Elser, J. J., and Hessen, D. O.: Stoichiometric relationships among producers, consumers and nutrient cycling in pelagic ecosystems, Biogeochemistry, 17, 49–67, 1992.
Sterner, R. W. and Elser, J. J.: Ecological stoichiometry: The biology of elements from molecules to the biosphere, Princeton University Press, 439 pp., 2002.
Straile, D.: Gross growth efficiencies of protozoan and metazoan zooplankton and their dependence on food concentration, predator-prey weight ratio, and taxonomic group, Limnol.

Oceanogr., 42, 1375–1385, 1997.
Thornton, D. C. O.: Diatom aggregation in the sea: mechanisms and ecological implications, Eur. J. Phycol., 37, 149–161, 2002.
Tyrrell, T.: The relative influences of nitrogen and phosphorus on oceanic primary production, Nature, 400, 525–531, 1999.
Uye, S. and Matsuda, O.: Phosphorus content of zooplankton from the Inland Sea of Japan, J. Oceanogr., 44, 280–286, 1988.
Uye, S. and Kaname, K.: Relations between fecal pellet volume and body size for major zooplankters of the Inland Sea of Japan, J. Oceanogr., 50, 43–49, 1994.
Van Cappellen, P. and Ingall, E. D.: Redox stabilization of the atmosphere and oceans by phosphorus-limited marine productivity, Science, 271, 493–496, 1996.
Vincent, D., Slawyk, G., L'Helguen, S., Sarthou, G., Gallinari, M., Seuront, L., Sautour, B., and Ragueneau, O.: Net and gross incorporation of nitrogen by marine copepods fed on ^{15}N-labelled diatoms: Methodology and trophic studies, J. Exp. Mar. Biol. Ecol., 352, 295–305, 2007.
Vitousek, P. M. and Howarth, R. W.: Nitrogen limitation on land and in the sea: How can it occur?, Biogeochemistry, 13, 87–115, 1991.
Von Bodungen, B.: Phytoplankton growth and krill grazing during spring in the Bransfield Strait, Antarctica–Implications from sediment trap collections, Polar Biol., 6, 153–160, 1986.
Walve, J. and Larsson, U.: Carbon, nitrogen and phosphorus stoichiometry of crustacean zooplankton in the Baltic Sea: implications for nutrient recycling, J. Plankton Res., 21, 2309–2321, 1999.
White, A. E., Spitz, Y. H., Karl, D. M., and Letelier, R. M.: Flexible elemental stoichiometry in *Trichodesmium* spp. and its ecological implications, Limnol. Oceanogr., 51, 1777–1790, 2006.
Wu, J., Sunda, W., Boyle, E. A., and Karl, D. M.: Phosphate depletion in the western North Atlantic Ocean, Science, 289, 759–762, 2000.
Yool, A. and Tyrrell, T.: Role of diatoms in regulating the ocean's silicon cycle, Glob. Biogeochem. Cy., 17, 1103, doi:10.1029/2002gb002018, 2003.

Table 1. Definitions of model parameters, values and literature sources.

Symbol	Parameter	Unit	Value
Extended Tyrrell model			
T_{vol}	Total volume of the ocean	m^{-3}	1.35×10^{18} [a]
T_{area}	Total surface area of the ocean	m^{-2}	3.62×10^{14} [a]
SD	Surface layer depth	m	500[a]
DD	Deep layer depth	m	3230[a]
K	Mixing coefficient between SD and DD	$m\,yr^{-1}$	3[a]
SF	Sedimentation fraction of TPP	%	0.3[e]
SR_0	Fraction of TPP remineralized in surface	%	95[a]
DR_0	Fraction of TPP remineralized in deep	%	(1-SR_0-SF)
SR_1	Fraction of total zooplankton productivity remineralized in surface	%	95
DR_1	Fraction of total zooplankton productivity remineralized in deep	%	(1-SR_1-SF)
SE_1	Fraction of zooplankton excretion in surface	%	90
DE_1	Fraction of zooplankton excretion in deep	%	(1-SE_1)
DN	Fraction of TPP of N that is regenerated via denitrification to N_2	%	1.5[a]
AN	Atmospheric input of N	$mol\,N\,m^{-2}\,yr^{-1}$	7.5×10^{-3} [a]
RP	Riverine input of P	$mol\,P\,m^{-2}\,yr^{-1}$	2×10^{-4} [a]
RN	Riverine input of N	$mol\,N\,m^{-2}\,yr^{-1}$	6.0×10^{-3} [a]
μ'_{NF}	Maximum growth rate of N_2-fixing phytoplankton	yr^{-1}	87.6[a]

References:
[a] Tyrrell (1999),
[b] Straile (1997),
[c] Hirst and Kiørboe (2002),
[d] Anderson et al. (2005),
[e] Sarmiento and Gruber (2006),
[f] Hutchins et al. (2007),
[g] Calbet and Landry (2004), Landry and Calbet (2004), Nejstgaard et al. (2007),
[h] Redfield (1934),
[i] Le Borgne (1982), Ikeda and Mitchell (1982), Walve and Larsson (1999), Gismervik (1997), Uye and Kaname (1994), Iguchi and Ikeda (2004).

BGD
7, 111–164, 2010

Table 1. Continued.

Symbol	Parameter	Unit	Value
μ'_O	Maximum growth rate of other phytoplankton	yr^{-1}	91.25[a]
K_P	Half-saturation constant for growth on PO_4	mol P m^{-2}	3×10^{-5} [a]
K_N	Half-saturation constant for growth on NO_3	mol N m^{-2}	5×10^{-4} [a]
M_0	Mortality rate of phytoplankton	yr^{-1}	73[a]
M_1	Mortality rate of zooplankton	yr^{-1}	20[c]
R^{NF}_{org}	N:P ratio in N_2-fixing phytoplankton biomass	mol/mol	33[f]
R^{O}_{org}	N:P ratio in other phytoplankton biomass	mol/mol	16[h]
R^{Z}_{org}	N:P ratio in zooplankton biomass	mol/mol	25[i]
Extended Sterner model			
a^{NF}_P	Accumulation efficiency of P in N_2-fixers of zooplankton	–	calculated
a^{NF}_N	Accumulation efficiency of N in N_2-fixers of zooplankton	–	calculated
a^{O}_P	Accumulation efficiency of P in other phytoplankton of zooplankton	–	calculated
a^{O}_N	Accumulation efficiency of N in other phytoplankton of zooplankton	–	calculated
L_m	Maximum accumulation efficiency of zooplankton	dimensionless	0.75[b]
β^P_1	Assimilation efficiency of P by zooplankton	dimensionless	0.80[d]
β^N_1	Assimilation efficiency of N by zooplankton	dimensionless	0.69[d]
ε_0	Fraction of phytoplankton natural mortality due to zooplankton predation	dimensionless	0.80[g]

References:
[a] Tyrrell (1999),
[b] Straile (1997),
[c] Hirst and Kiørboe (2002),
[d] Anderson et al. (2005),
[e] Sarmiento and Gruber (2006),
[f] Hutchins et al. (2007),
[g] Calbet and Landry (2004), Landry and Calbet (2004), Nejstgaard et al. (2007),
[h] Redfield (1934),
[i] Le Borgne (1982), Ikeda and Mitchell (1982), Walve and Larsson (1999), Gismervik (1997), Uye and Kaname (1994), Iguchi and Ikeda (2004).

BGD
7, 111–164, 2010

Table 2. Comparison of model solutions at steady-state with values from the literature.

Variable	Unit	Model result	Literature
NF*, Nitrogen-fixer	Tmol N	0.08	–
(NF+O)*, Phytoplankton	Tmol N	8.46	7.5–10.7[d, e, f]
H_1^*, Zooplankton	Tmol N	12.89	4.38[*,a], 8.1[o]
P_S^*, Surface phosphate	mmol P m^{-3}	0.15	1.08[b]
N_S^*, Surface nitrate	mmol N m^{-3}	1.98	13.50[b]
P_D^*, Deep phosphate	mmol P m^{-3}	2.50	2.17[b]
N_D^*, Deep nitrate	Mmol N m^{-3}	30.67	31[b]
R_S^*, Surface N:P ratio	mol/mol	13.4	12.5[b]
R_D^*, Deep N:P ratio	mol/mol	12.24	14.3[b]
Total primary production	Gt C yr^{-1}	48.97	36–50[c,d], 46–61[h]
Denitrification	Gt N yr^{-1}	0.65 (1.5% of TPP)	0.9–2% of TPP[l]
Export across 500 m	Gt C yr^{-1}	2.45 (5% of TPP)	3–25% of TPP[f, i, h]
Burial	Gt C yr^{-1}	0.15 (0.3% of TPP)	0.1–0.3% of TPP[g, h]
Secondary primary production	Gt N yr^{-1}	6.9 (80% of TPP)	70–80% of TPP[j, k]
Zooplankton excretion (N and P)	Gt N yr^{-1}	1.19	1.18–2.38[a]
Zooplankton mortality	Gt N yr^{-1}	3.6	2.24***
Zooplankton GEE for N	%	52, 45**	30[n]
Zooplankton GEE for P	%	33, 60**	7–90[m]

References:
[a] Hernandéz-Leon et al. (2008), [b] Garcia et al. (2006),
[c] Longhurst (1995), [d] Antoine et al. (1996),
[e] Barnes and Hughes (1999), [f] Schlesinger (1977),
[g] Mackenzie et al. (1993), [h] Dunne et al. (2007),
[i] Tyrrell (1999), [j] Calbet (2001),
[k] Calbet and Landry (2004), [l] Gruber (2008),
[m] DeMott et al. (1998), [n] Vincent et al. (2007),
[o] Gasol et al. (1997).
Notes:
* net epipelagic Mesozooplankton,
** for O and NF respectively,
*** estimation based on estimates of zooplankton mortality rate by Hirst and Kiørboe (2002) and of net epipelagic mesozooplankton biomass by Hernandéz-Leon et al. (2008).

BGD
7, 111–164, 2010

Table 3. Sensitivity of the deep nutrient concentrations to model parameters. Values represent the mean sensitivity index (SI, %) as a percentage of variation of model solutions compared to the standard simulation when a parameter has been decreased by 50%. See text for details on the calculation of SI.

Model parameter	N_D	P_D	$N_D : P_D$
DR_0	10	9	1
DR_1	29	23	10
SE_1	11	13	12
DN	4	<1	4
β_1^N	1	<1	1
β_1^P	15	16	2
L_m	32	30	1
ε_0	15	16	3
R_{org}^Z	8	8	1
K	92	91	3

Table 4. Ecological C:N:P stoichiometry of various marine pelagic invertebrates and vertebrates (mean and standard deviation in brackets).

	C:N	C:P	N:P	Reference(s)
Microzooplankton	–	–	21.50 (2.10)	h
Copepods	5.54 (1.60)	131.80 (60.80)	23.32 (9.35)	b, c, d, e, f
Euphausids-mysids	4.58 (0.48)	120.20 (31.20)	26.15 (6.81)	a, b, c
Other crustacea	5.43 (0.23)	94.18 (10.64)	17.35 (1.72)	b, e, f
Chaetognaths	4.16 (0.07)	124.99 (12.32)	30.06 (3.45)	b, d
Salps	4.39 (0.26)	148.99 (19.92)	34.14 (6.52)	c, g, h
Polychaetes	4.49 (0.52)	178.30 (91.90)	38.38 (16.79)	b, c
Mollusks	4.80	162.30	33.84	c
Siphonophores	4.28	200.00	46.72	b
Hydromedusae	2.91	108.70	37.40	b
Pteropods	8.15	196.08	24.06	b
Fish and fish larvae	4.57	69.93	15.31	b

References:
[a] Roger (1978);
[b] Beers (1978): means from monthly surveys off Bermuda (North Atlantic);
[c] Ikeda and Mitchell (1982): Southern Ocean;
[d] Uye and Matsuda (1988): Japan Sea;
[e] Gismervik (1997): Oslofjord, Norway;
[f] Walve and Larson (1999): Baltic Sea;
[g] Igushi and Ikeda (2004): Southern Ocean;
[h] Le Borgne (1982): off the Guinea coast.

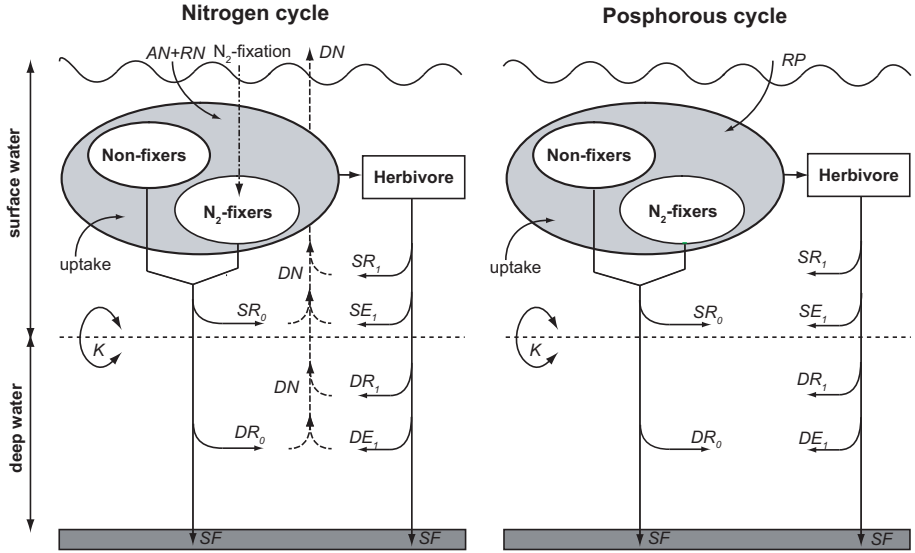

Fig. 1. A modified version of Tyrell's 2-box model of N and P cycling in the ocean which includes a parameterisation of herbivores. The model parameter abbreviations are described in Table 1.

BGD
7, 111–164, 2010

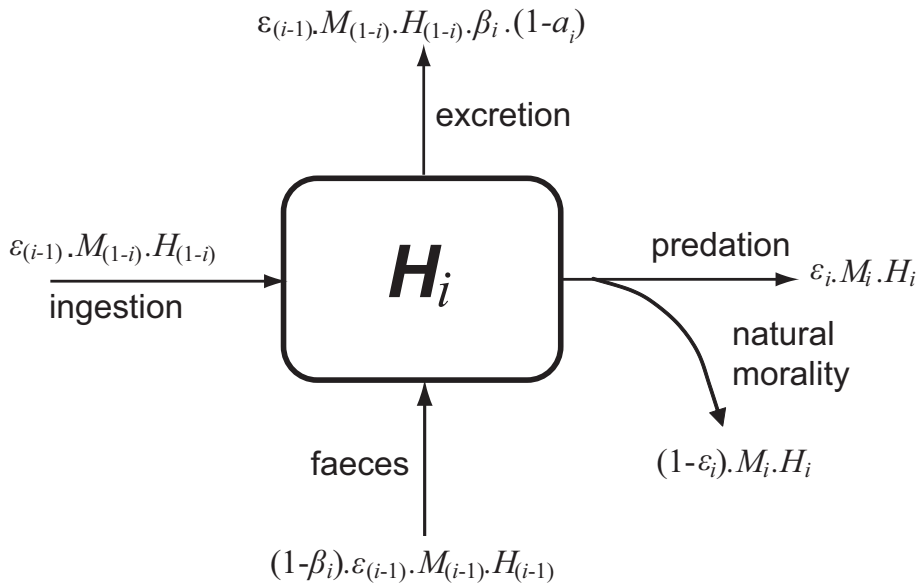

Fig. 2. Flow diagram for a trophic level i (H_i); ε_i represents the proportion of the annual natural mortality rate (M_i) which is associated to predation by the trophic level $H_{(i+1)}$; β_i represents the assimilation efficiency and $(1-\beta_i)$ represents the proportion of ingested food which is not incorporated into biomass.

BGD
7, 111–164, 2010

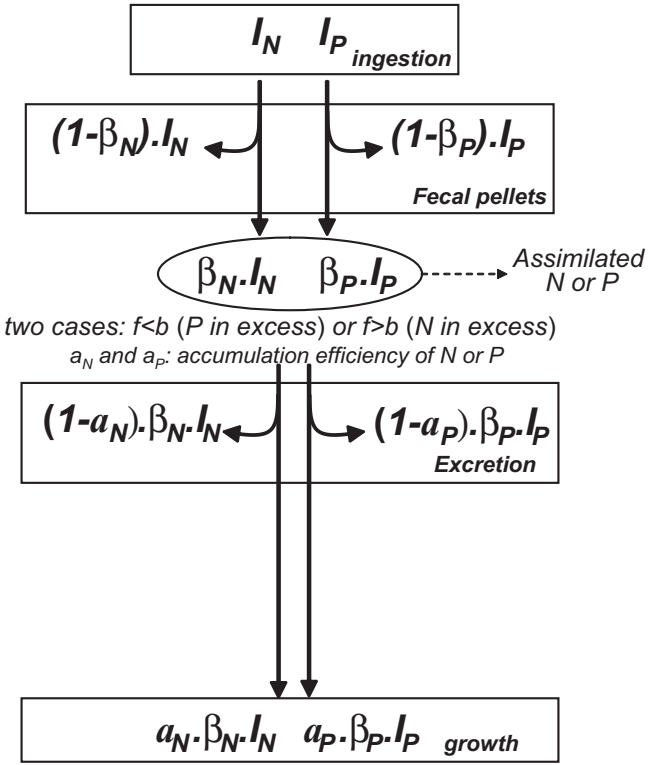

Fig. 3. Fluxes of N and P in herbivores. I_i is the ingestion, β_i is the assimilation efficiency, and a_i is the accumulation efficiency (i=N or P).

BGD
7, 111–164, 2010

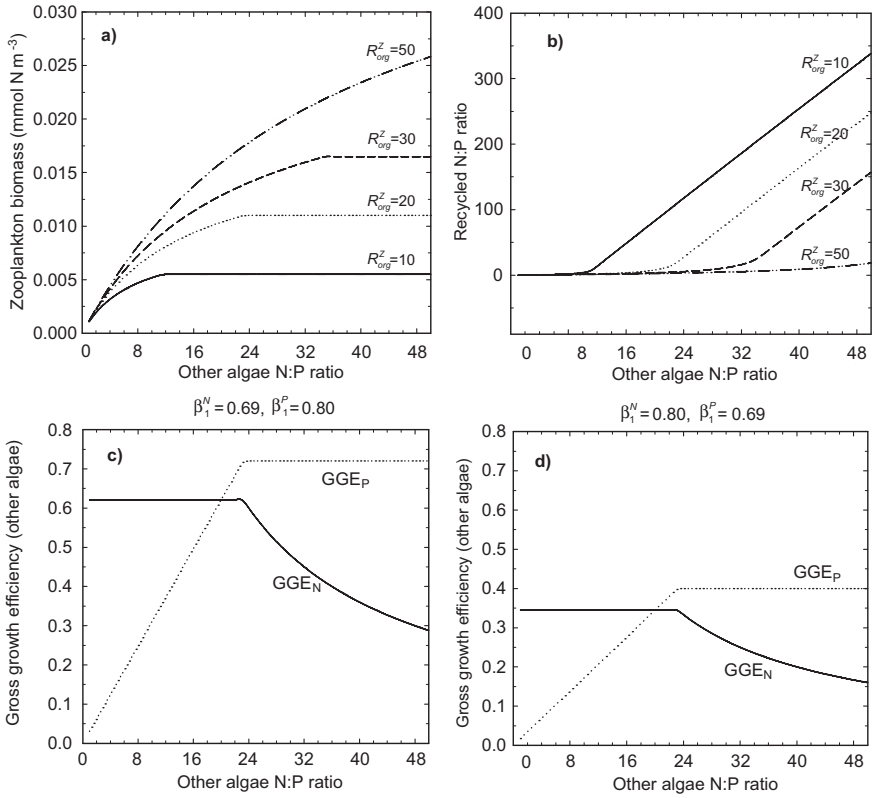

Fig. 4. **(a)** Global herbivore biomass (mmol N m^{-3}) plotted against the ratio of nitrogen to phosphorus (N:P) in non-fixers, using four different N:P ratios in herbivores; **(b)** The N:P ratio of the products released by herbivores plotted against the N:P ratio in non-fixers; **(c)** and **(d)** Gross growth efficiency of N (GGE_N) and P (GGE_P) plotted against the N:P ratio in non-fixers (R^O_{org}), using two set of assimilation efficiencies: (c) $\beta_1^N = 0.69$ and $\beta_1^N = 0.80$, (d) vice-versa.

BGD
7, 111–164, 2010

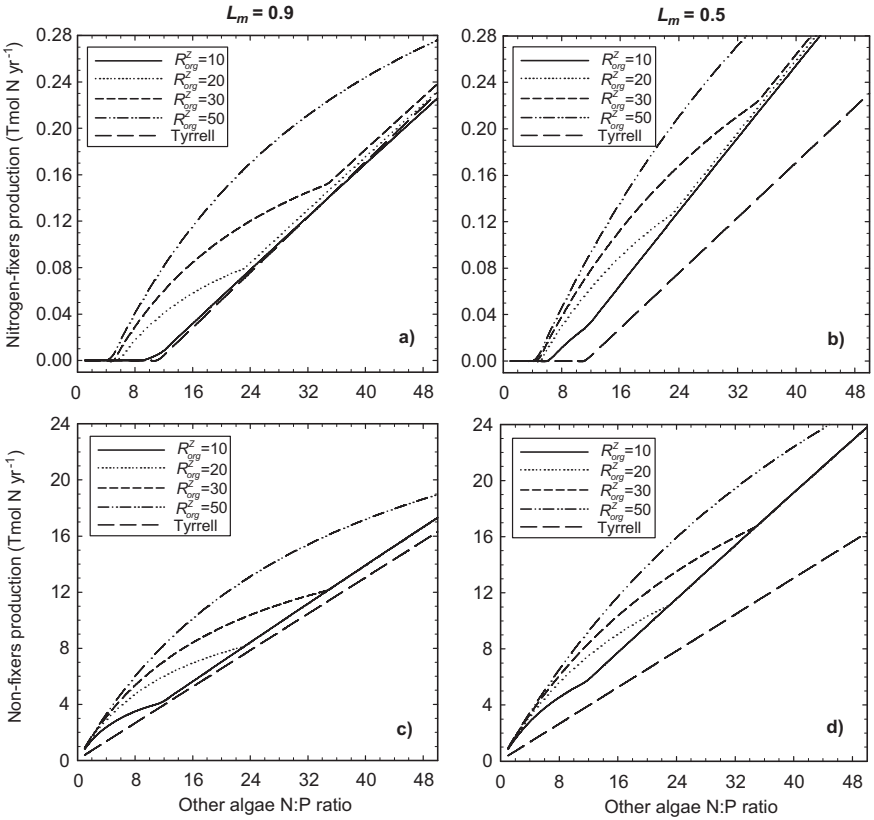

Fig. 5. **(a)** and **(b)** N_2-fixation plotted against the ratio of nitrogen to phosphorus (N:P) in non-fixers using two different maximum accumulation efficiencies for herbivores (L_m=0.9 or L_m=0.5), and four different N:P ratios in herbivores (R^Z_{org}). The assimilation efficiency of nitrogen (β_1^N) and phosphorus (β_1^P) were set at 0.69 and 0.80, respectively. **(c)** and **(d)** same as (a) and (b), but for non-fixers. Solutions for the Tyrell's model without herbivores are also shown (dashed line).

BGD
7, 111–164, 2010

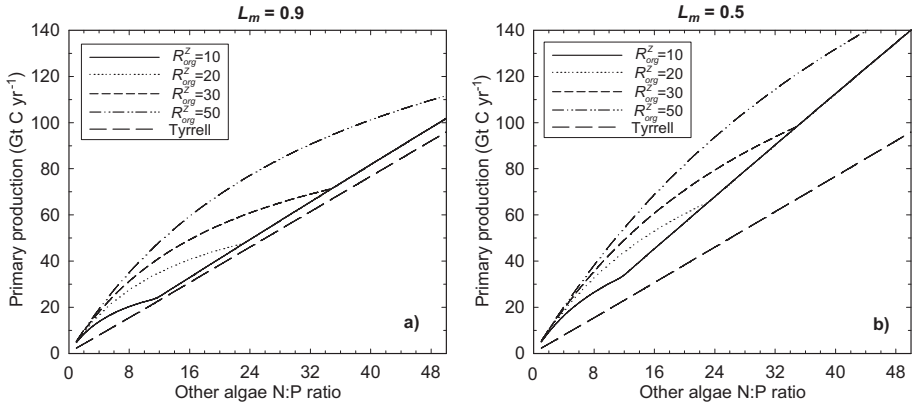

Fig. 6. Global primary production plotted against the ratio of nitrogen to phosphorus (N:P) in non-fixers pool using two different maximum accumulation efficiencies in herbivores (L_m=0.9 or L_m=0.5), and four different N:P ratios in herbivores (R^Z_{org}). The assimilation efficiency of nitrogen (β^N_1) and phosphorus (β^P_1) were set at 0.69 and 0.80, respectively. Solutions for the Tyrell's model without herbivores are also shown (dashed line).

BGD
7, 111–164, 2010

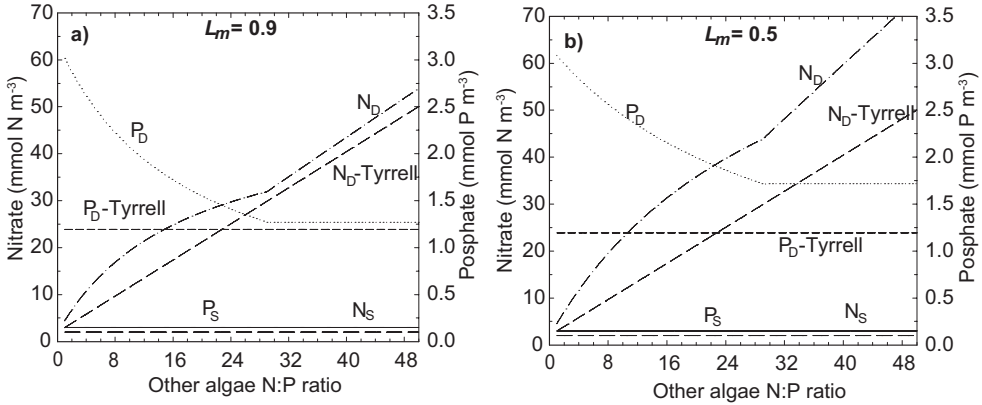

Fig. 7. Nutrient concentrations plotted against the N:P ratio in non-fixers using the default parameters set listed in Table 1, except for L_m.

BGD
7, 111–164, 2010

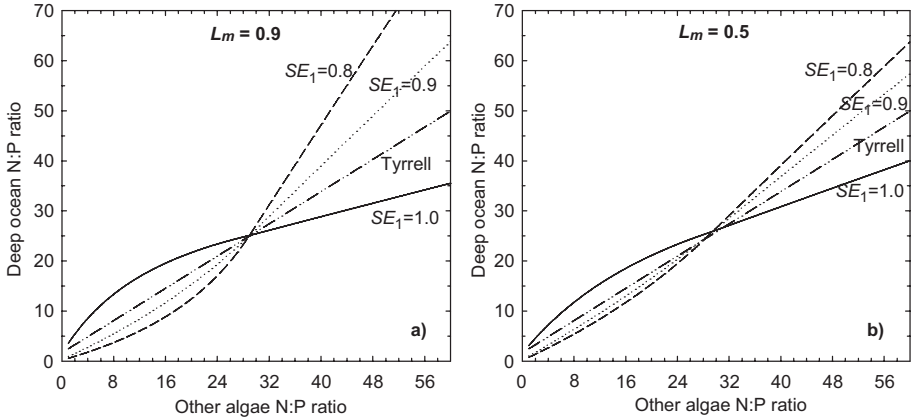

Fig. 8. Simulated deep ocean N:P ratio vs. non-fixers N:P ratio (R^{O}_{org}), using a maximum accumulation efficiency for herbivores of **(a)** L_m=0.9 and **(b)** L_m=0.5. Different values of the fractions of excretion occuring in the surface of the ocean (SE_1) were also used. Parameters other than L_m, R^{O}_{org} and SE_1 are kept similar with base run (Table 1).

BGD
7, 111–164, 2010

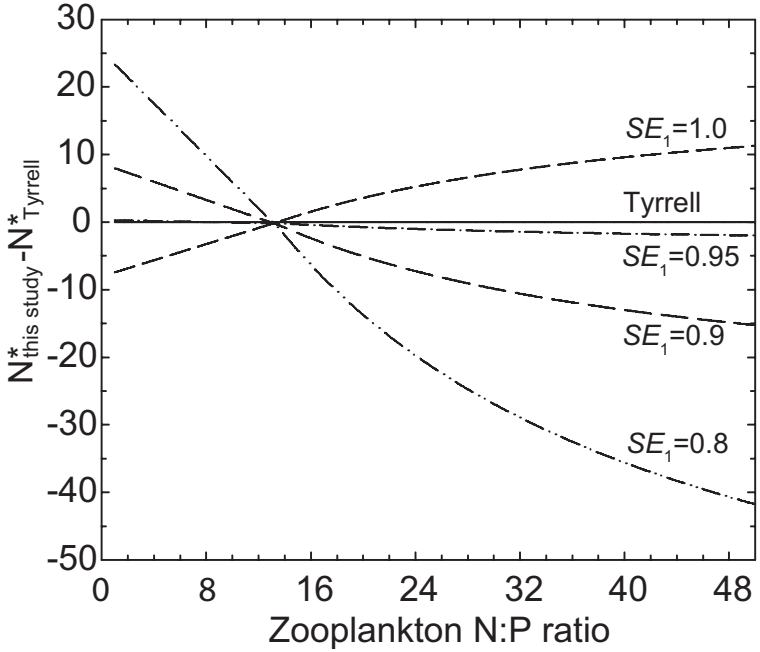

Fig. 9. Estimated deep ocean N* plotted against the N:P ratio in herbivores (R^Z_{org}), using different fraction of herbivore excretion occuring in the surface layer (SE_1 = 0.80, 0.90, 0.95 or 1.0). Parameters other than R^Z_{org} and SE_1 are kept similar with base run (Table 1). The N* value was corrected from N* in Tyrrell's original model without herbivores.

BGD
7, 111–164, 2010